Anisotropies in the arrival direction of ultrahigh-energy cosmic rays measured by the Pierre Auger Observatory

PIERRE AUGER OBSERVATORY

Ugo Giaccari [a], on behalf the Pierre Auger Collaboration [b]

[a] IMAPP, Radboud University Nijmegen, Nijmegen, The Netherlands
[b] Observatorio Pierre Auger, Av. San Martín Norte 304, 5613 Malargüe, Argentina

Directional analyses at the Pierre Auger Observatory

Two lines of analyses since the beginning of our data taking

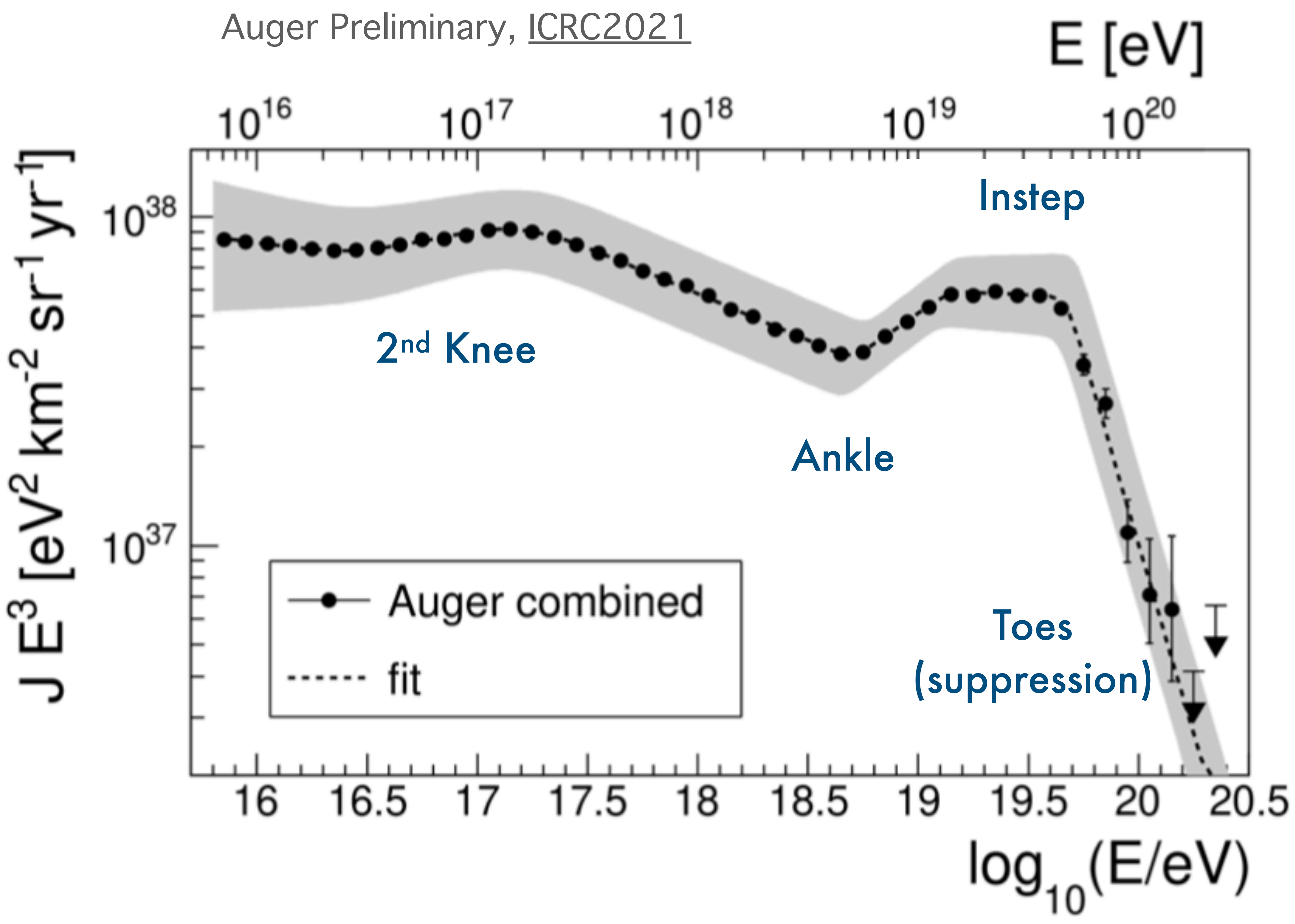

Large scale anisotropies can be present at all energies

- Propagation from extragalactic sources distributed anisotropically
- Diffusion from individual extragalactic sources
- Diffusive escape from Galaxy of CRs from Galactic sources
- Compton-Getting effect due to the Earth motion in the CR rest frame

Method: Rayleigh analysis in right ascension (and declination)

Challenge: control exposure and event rate down below < % level

Small-intermediate scale anisotropies can be present in the suppression region

- At UHE, cosmic rays have reduced horizon and maybe enough rigidity ***to point back to their sources***

Method: Comparison of UHECR arrival directions with astronomical objects

Challenge: control of exposure and trial factor (energy, angle…)

Anisotropy studies over three decades in energy, from below the 2nd Knee to the suppression region

The Observatory and the data set

From Surface Detector data ≈ 100% duty cycle (larger statistics), simpler exposure

for an anisotropy search with the Fluorescence Detector data

see Eric Mayotte's talk (this session)

Surface Detector: 1660 water-Cherenkov detectors (WCDs) on a triangular grid

► **SD-1500: spacing 1500 m**

- 1500 m vertical reconstruction (0º ≤ θ < 60º), full efficiency E ≥ 2.5 EeV
- 1500 m inclined reconstruction (60º ≤ θ ≤ 80º), full efficiency E ≥ 4 EeV

► **SD-750: spacing 750 m**

- 750 m vertical reconstruction (0º ≤ θ ≤ 55º), full efficiency E ≥ 0.3 EeV

► **Fluorescence Detector (FD)** → 27 telescopes in four buildings

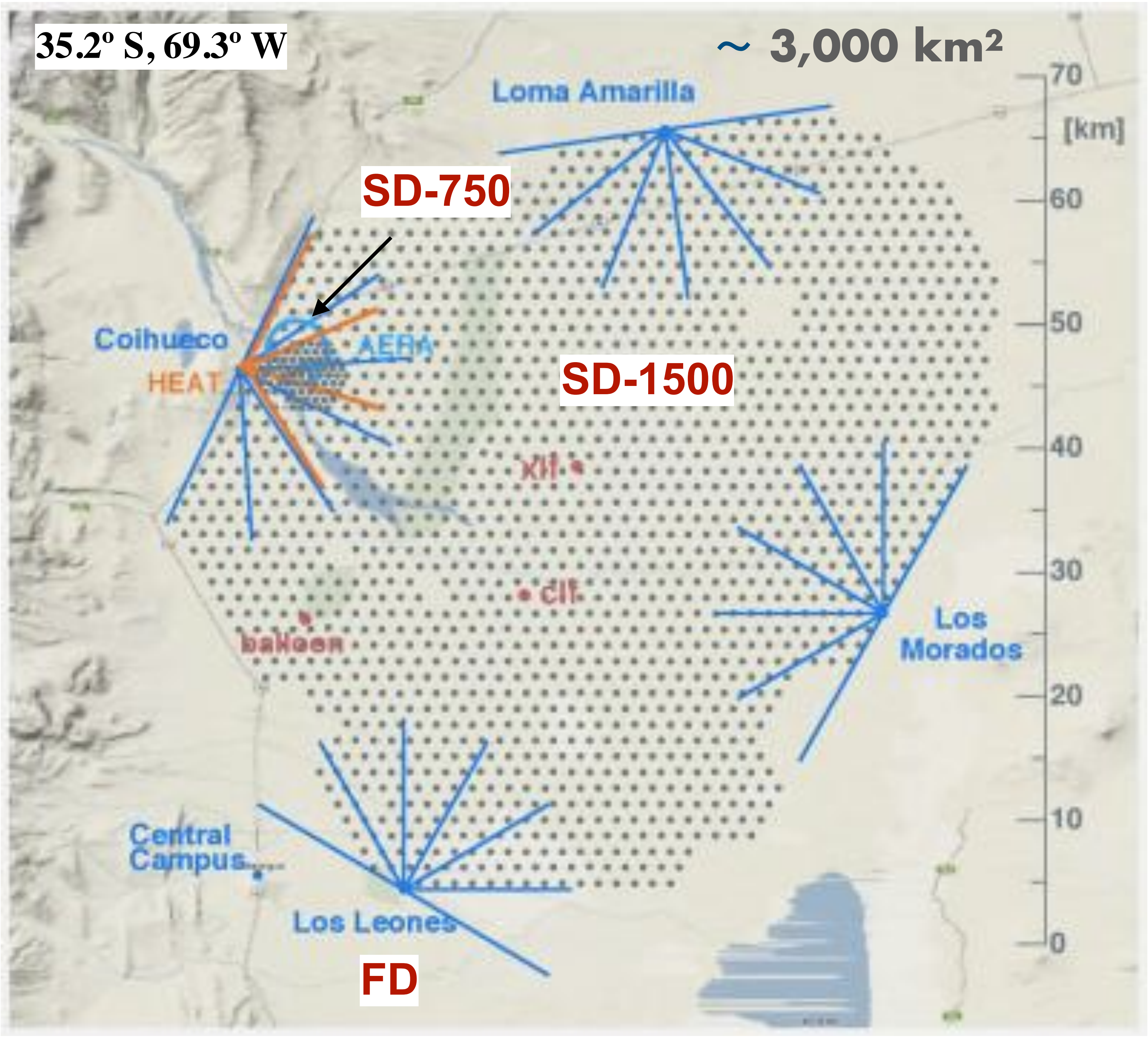

(see Quentin Luce's talk)

Optimized quality cuts for each analysis and energy range

- Large scale anisotropies above 0.03 EeV up to 4 EeV → SD-750 + SD-1500 vertical data (up August 2018), **≈ 92,500 km² sr yr**, sky coverage ≈ 70%
- Large scale anisotropies above 4 EeV → SD-1500 vertical + inclined events (up to the end 2020), **≈ 110,000 km² sr yr**, **sky coverage ≈ 85%**
- Small scale anisotropies above 32 EeV → SD-1500 vertical + inclined events (up to the end 2020), **≈ 122,000 km² sr yr**, **sky coverage ≈ 85%**

more than 2,600 events above 32 EeV

Different reconstructions, different spacing but similar angular resolution: ≈ 1˚ for the arrival direction. Energy resolution 7%-16%

Same energy scale, calibrated with the fluorescence detector: ≈ 14% systematic uncertainty

Control of the counting rate

Additional challenge for directional analyses: *control of the event rate*

► Atmospheric effects ⟹ essential to search for anisotropies in RA

- Impact on e.m. component of the showers due to T and P variations. **Correction of the energy estimator on vertical events,** no correction on inclined events (mostly muons)

Pierre Auger Collab. 2017 JINST 12 P02006

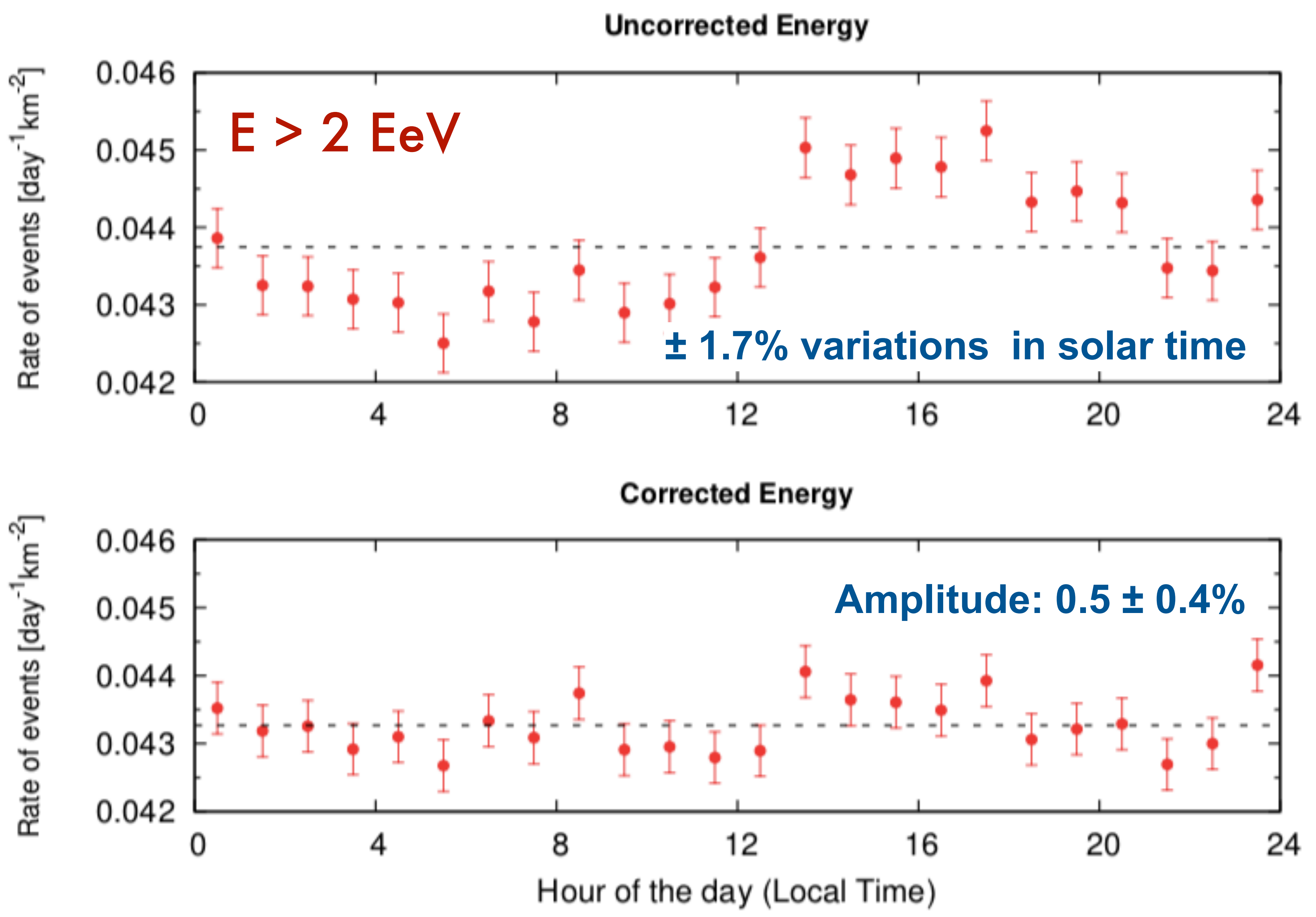

► Non uniformities of the exposure

- Effective aperture of the Observatory is not uniform in sidereal time.
If not accounted, spurious contribution to equatorial dipole well below 0.1%

► Geomagnetic effect ⟹ essential to search for anisotropies in declination

- Impact circular symmetry of the showers. Larger effect at high zenith angles. **Correction of the energy estimator on vertical events,** no correction on inclined events (accounted in reconstruction).

Pierre Auger Collab. JCAP11(2011)022

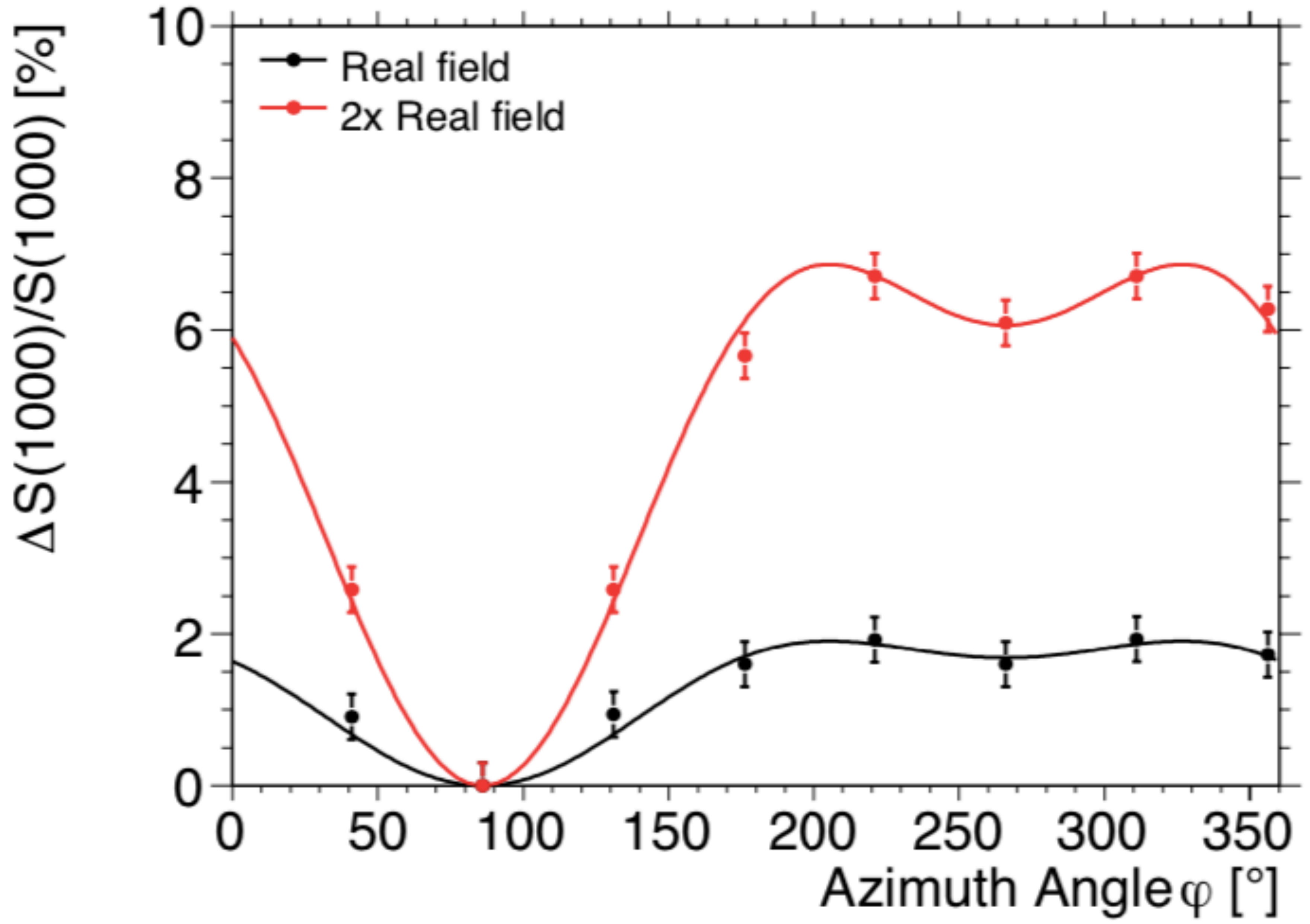

► Tilt of the Surface Detector

- Inclined on average 0.2º towards South-East.
If not accounted, spurious contribution to N-S dipole component of ∼ −0.4%

Large scale analysis: first harmonic analyses in RA

From below the 2nd knee to suppression region

Method: **Above 2 EeV, Rayleigh formalism** gives amplitude, phase (hour angle of the maximum intensity) and probability for detecting a spurious modulation due to a fluctuation of a uniform distribution [J. Linsley PRL 34 (175) 1530]. **Below 2 EeV, East-West method**: designed to subtract spurious effects (though with reduced sensitivity) [R. Bonino et al 2011 ApJ 738 67]

Pierre Auger Collab. Astrophys. J. 891 (2020) 142

► to compare between experiments, we use the equatorial dipole component

► all the energy bins < 8 EeV upper bound are at the level 1-3% at 99% CL

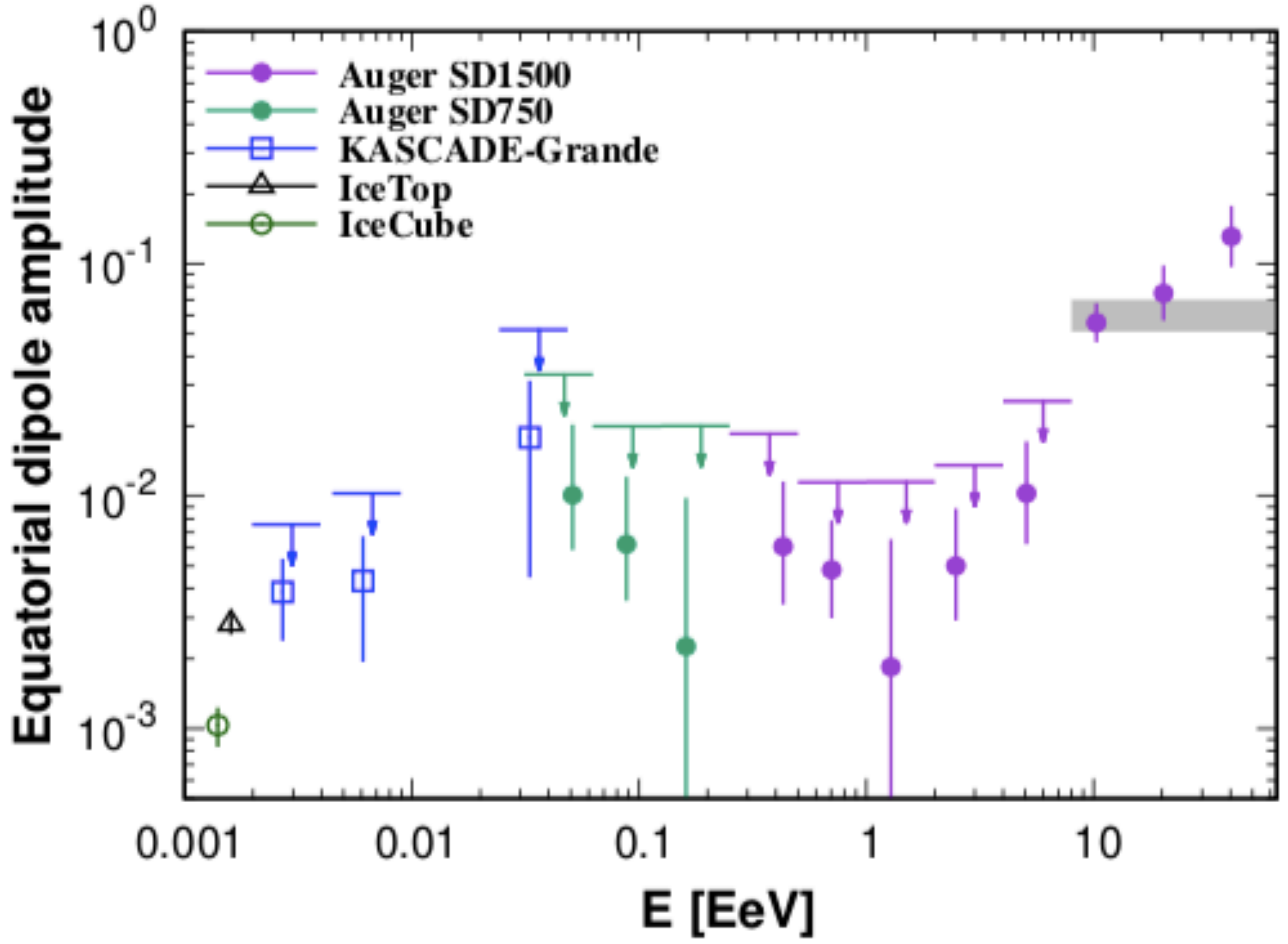

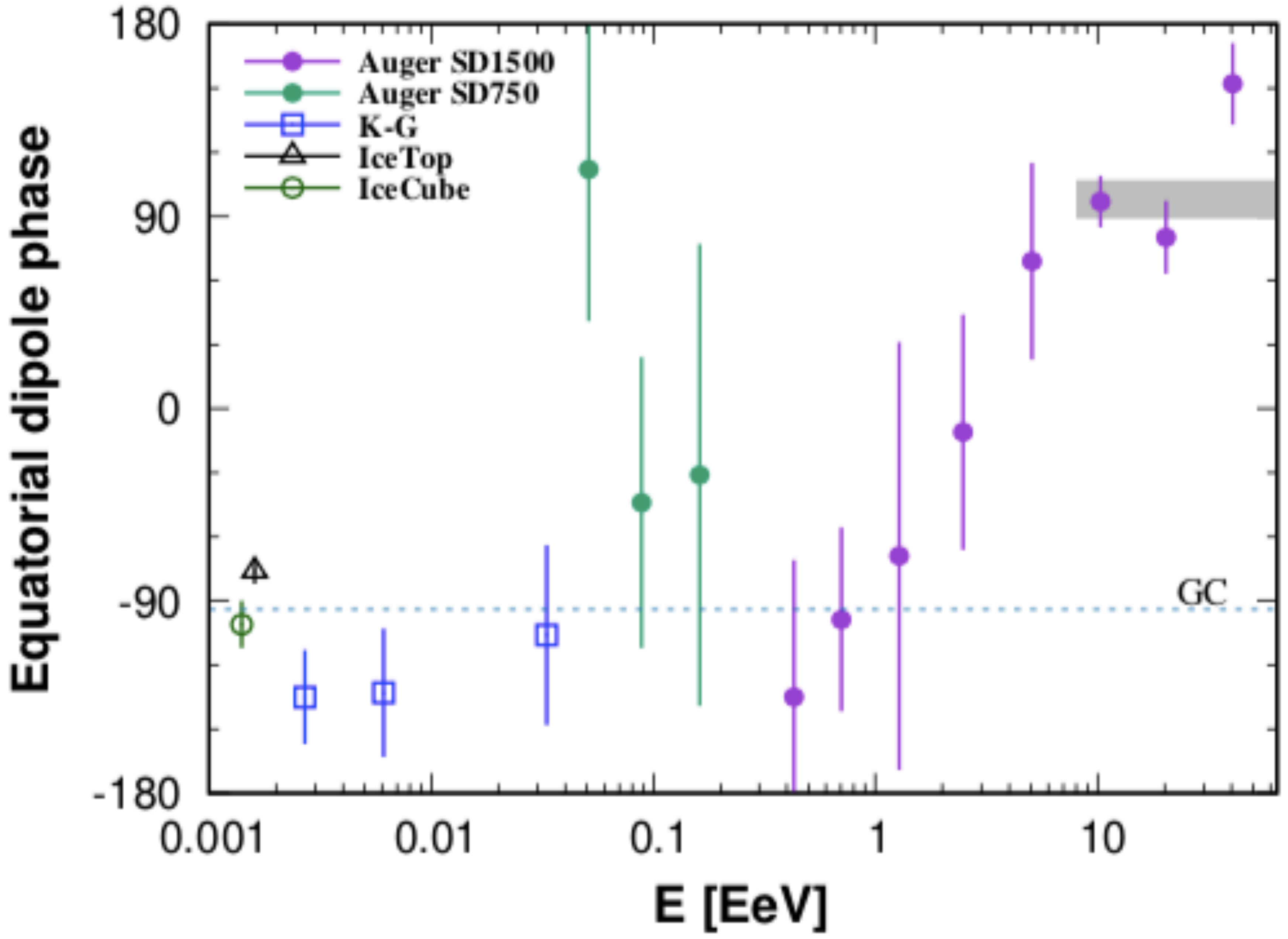

Amplitude grow: from below % to above 10%

Phase shift: from ~ GC to opposite direction

Suggests transition from anisotropies of Galactic origin below ~ 1 EeV to extragalactic origin above few EeV

First harmonic analyses above 4 EeV

E (EeV)	N	$d_\perp$	d_z	d	α_d [°]	δ_d [°]	$P(\geq r_1^\alpha)$
4-8	106, 290	$0.01^{+0.006}_{-0.004}$	-0.012 ± 0.008	$0.016^{+0.008}_{-0.005}$	97 ± 29	-48^{+23}_{-22}	1.4×10^{-1}
8-16	32, 794	$0.055^{+0.011}_{-0.009}$	-0.03 ± 0.01	$0.063^{+0.013}_{-0.009}$	95 ± 10	-28^{+12}_{-13}	3.1×10^{-7}
16-32	9, 156	$0.072^{+0.021}_{-0.016}$	-0.07 ± 0.03	$0.10^{+0.03}_{-0.02}$	81 ± 15	-43^{+14}_{-14}	7.5×10^{-4}
≥8	44, 398	$0.059^{+0.009}_{-0.008}$	-0.042 ± 0.013	$0.073^{+0.011}_{-0.009}$	95 ± 8	-36^{+9}_{-9}	5.1×10^{-11}
≥32	2, 448	$0.11^{+0.04}_{-0.03}$	-0.12 ± 0.05	$0.16^{+0.05}_{-0.04}$	139 ± 19	-47^{+16}_{-15}	1.0×10^{-2}

Pierre Auger Collab. ICRC2021

→ **at 6.6σ**

It was 1.4×10^{-9} in ApJ 868, 1 (2020)
2.6×10^{-8} in Science 357 (2017)
6×10^{-5} in ApJ 802, 111 (2015)

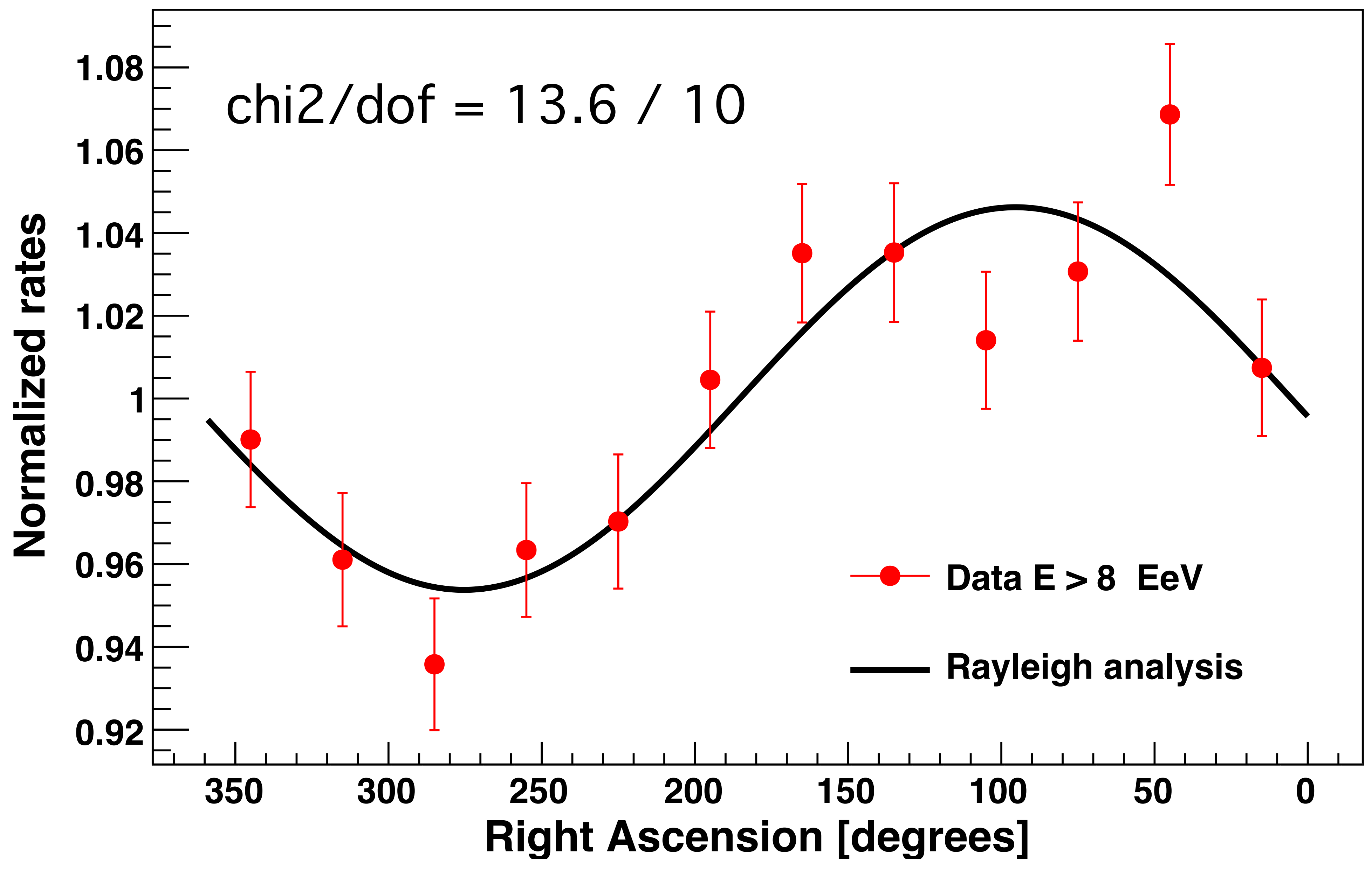

Significance of the first harmonic modulation became larger as the exposure increase

4-8 EeV bin: consistent with isotropy, $P(\geq r) = 1.4 \times 10^{-1}$

> 8 EeV bin: $P(\geq r) = 5 \times 10^{-11}$, $\alpha = 95° \pm 8°$

Evidence of large scale anisotropies above 8 EeV

(detection above 5σ accounting the null results in the other energy bins)

Dipole reconstruction

E (EeV)	N	$d_\perp$	d_z	d	$\alpha_d [^\circ]$	$\delta_d [^\circ]$	$P(\geq r_1^\alpha)$
4-8	106, 290	$0.01^{+0.006}_{-0.004}$	-0.012 ± 0.008	$0.016^{+0.008}_{-0.005}$	97 ± 29	-48^{+23}_{-22}	1.4×10^{-1}
8-16	32, 794	$0.055^{+0.011}_{-0.009}$	-0.03 ± 0.01	$0.063^{+0.013}_{-0.009}$	95 ± 10	-28^{+12}_{-13}	3.1×10^{-7}
16-32	9, 156	$0.072^{+0.021}_{-0.016}$	-0.07 ± 0.03	$0.10^{+0.03}_{-0.02}$	81 ± 15	-43^{+14}_{-14}	7.5×10^{-4}
≥8	44, 398	$0.059^{+0.009}_{-0.008}$	-0.042 ± 0.013	$0.073^{+0.011}_{-0.009}$	95 ± 8	-36^{+9}_{-9}	5.1×10^{-11}
≥32	2, 448	$0.11^{+0.04}_{-0.03}$	-0.12 ± 0.05	$0.16^{+0.05}_{-0.04}$	139 ± 19	-47^{+16}_{-15}	1.0×10^{-2}

assuming a pure dipolar contribution

> 8 EeV
dipole amplitude = 7.3%$^{+1.1\%}_{-0.9\%}$
direction α = 95º ± 8º, δ = -36º ± 9º

Flux sky map E > 8 EeV

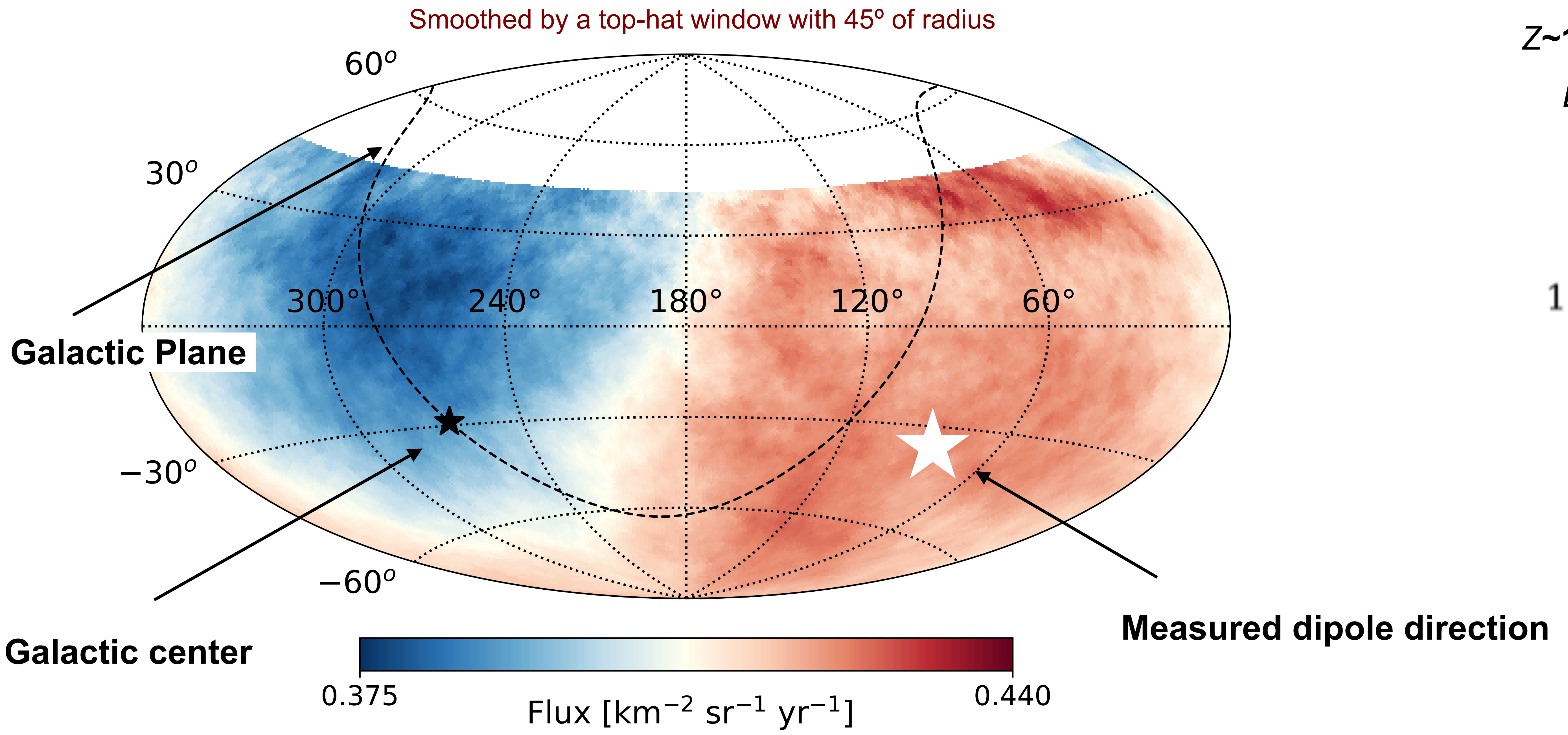

Equatorial coordinates

dipole directions in the Galactic scenario

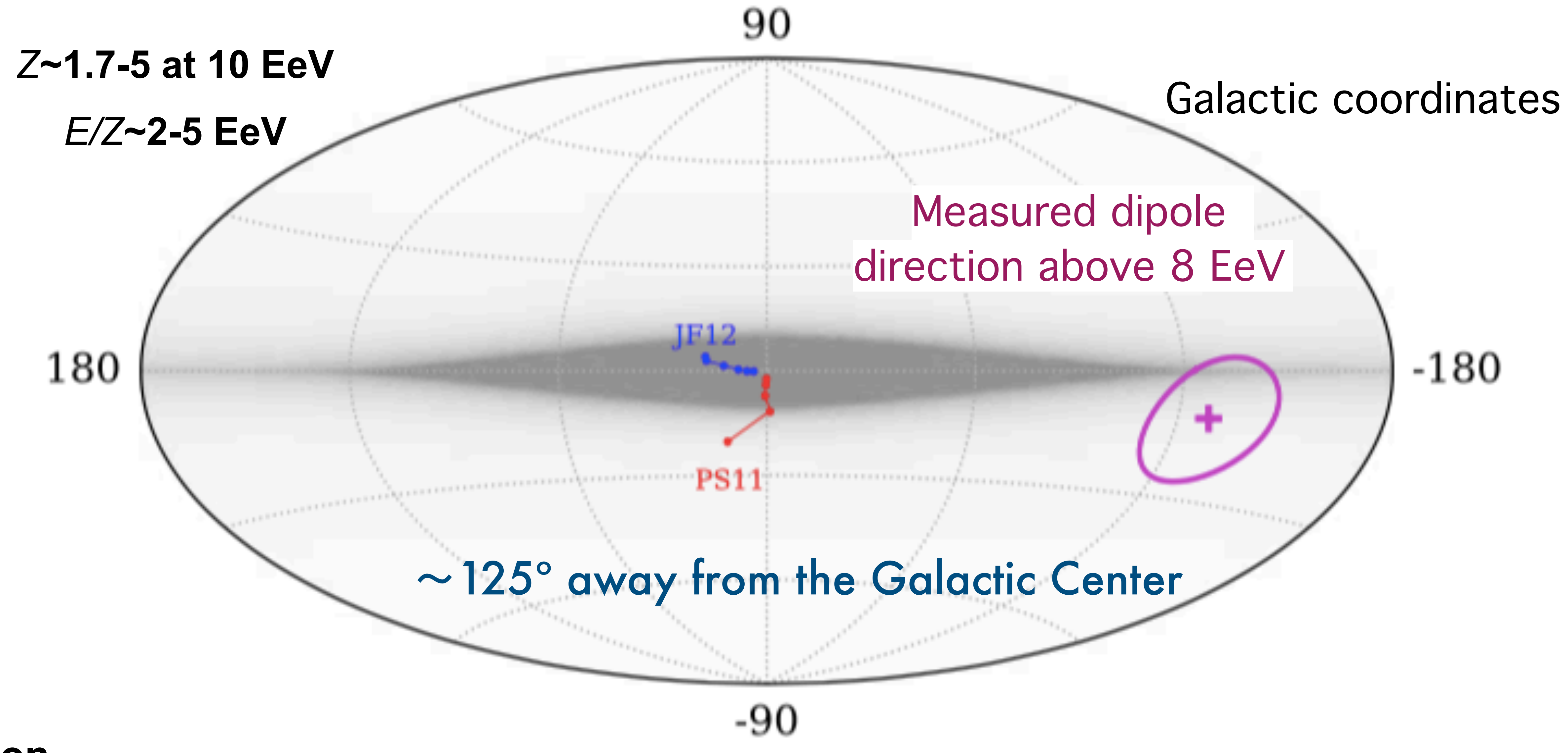

Extragalactic Origin

(Amplitude: factor 10 > CG effect due to the Earth motion in the CR rest frame)

Energy dependence of dipolar modulation

Dividing the E > 8 EeV bin into three

Dipole amplitudes above 4 EeV

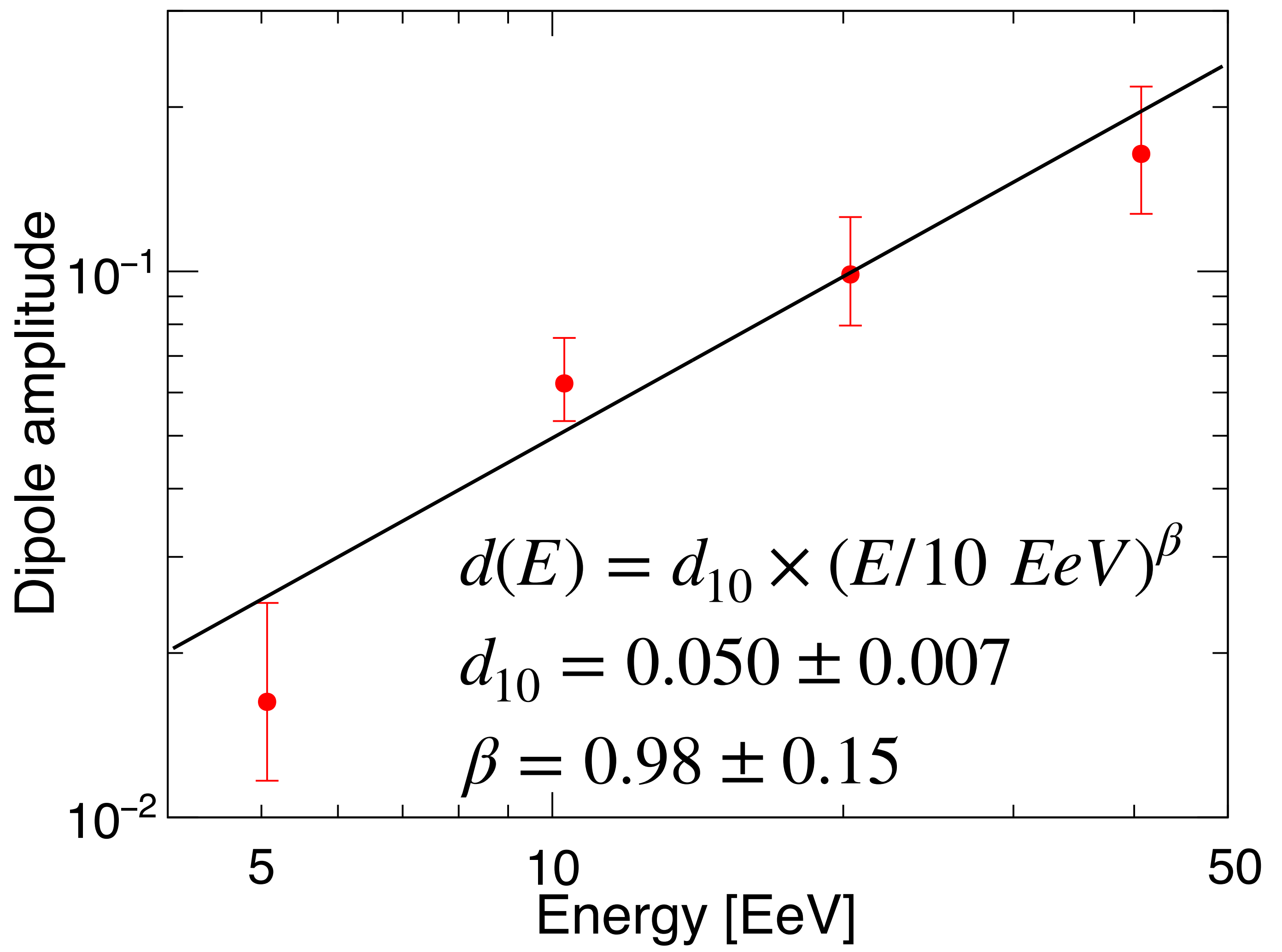

dipole amplitude increases with energy

(energy-independent fit disfavored above 5σ)

Pierre Auger Collab. ApJ 868, 1 (2020)

Pierre Auger Collab. ICRC2021

Dipole directions above 4 EeV

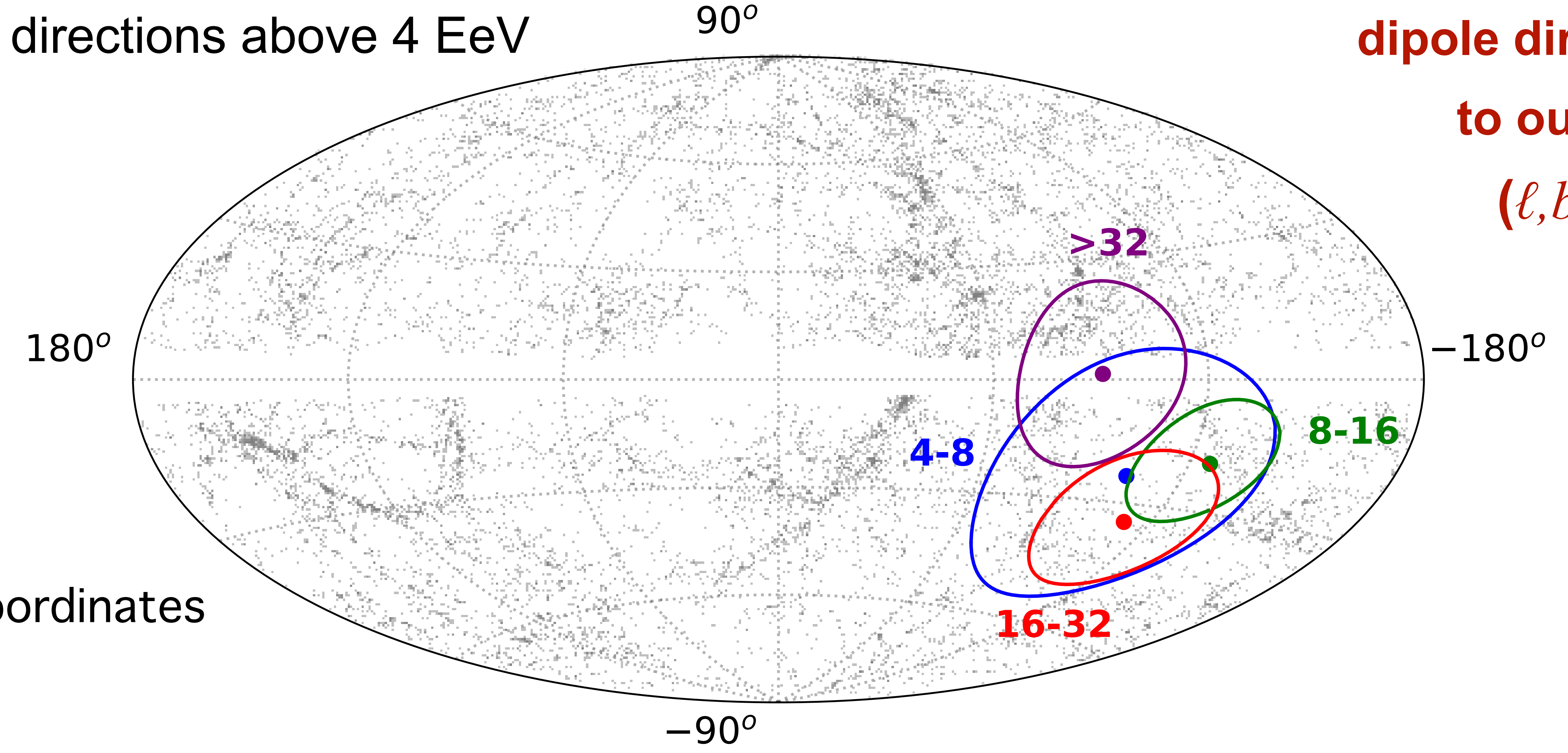

Galactic coordinates

dipole directions close to outer spiral arm

(ℓ,b) = (−100°, 0°)

Extragalactic Dipole and GMF

dipole direction after accounting for Galactic B field for E/Z = 32, 16, 8 and 4 EeV

Dipole direction Outside Galaxy

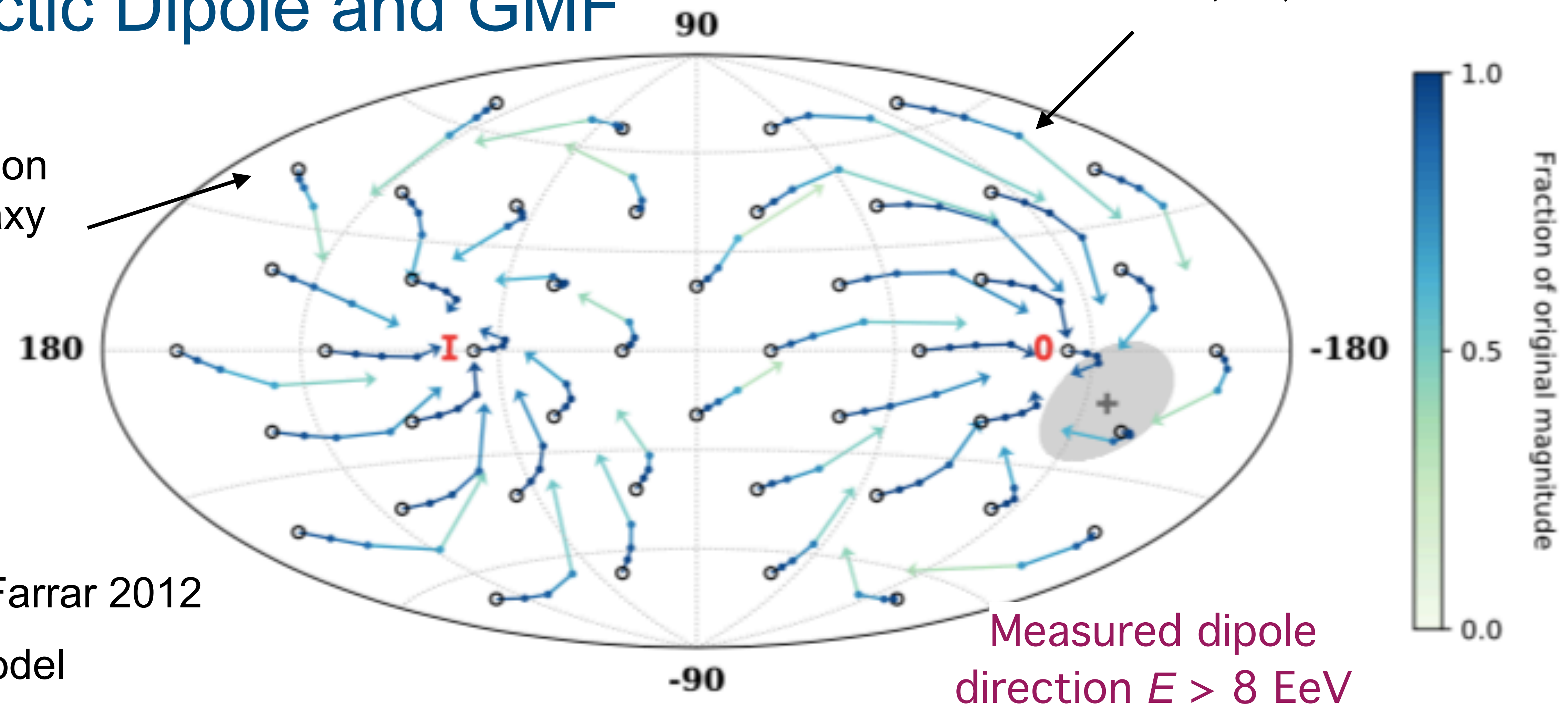

Measured dipole direction E > 8 EeV

using Jansson&Farrar 2012 B field model

Extragalactic dipole direction gets shifted towards spiral arms

Arrival directions above 32 EeV

Pierre Auger Collab. The Astrophys. J. 935 (2022)170

Search for localized excesses

not specifying a priori the targeted regions of the sky

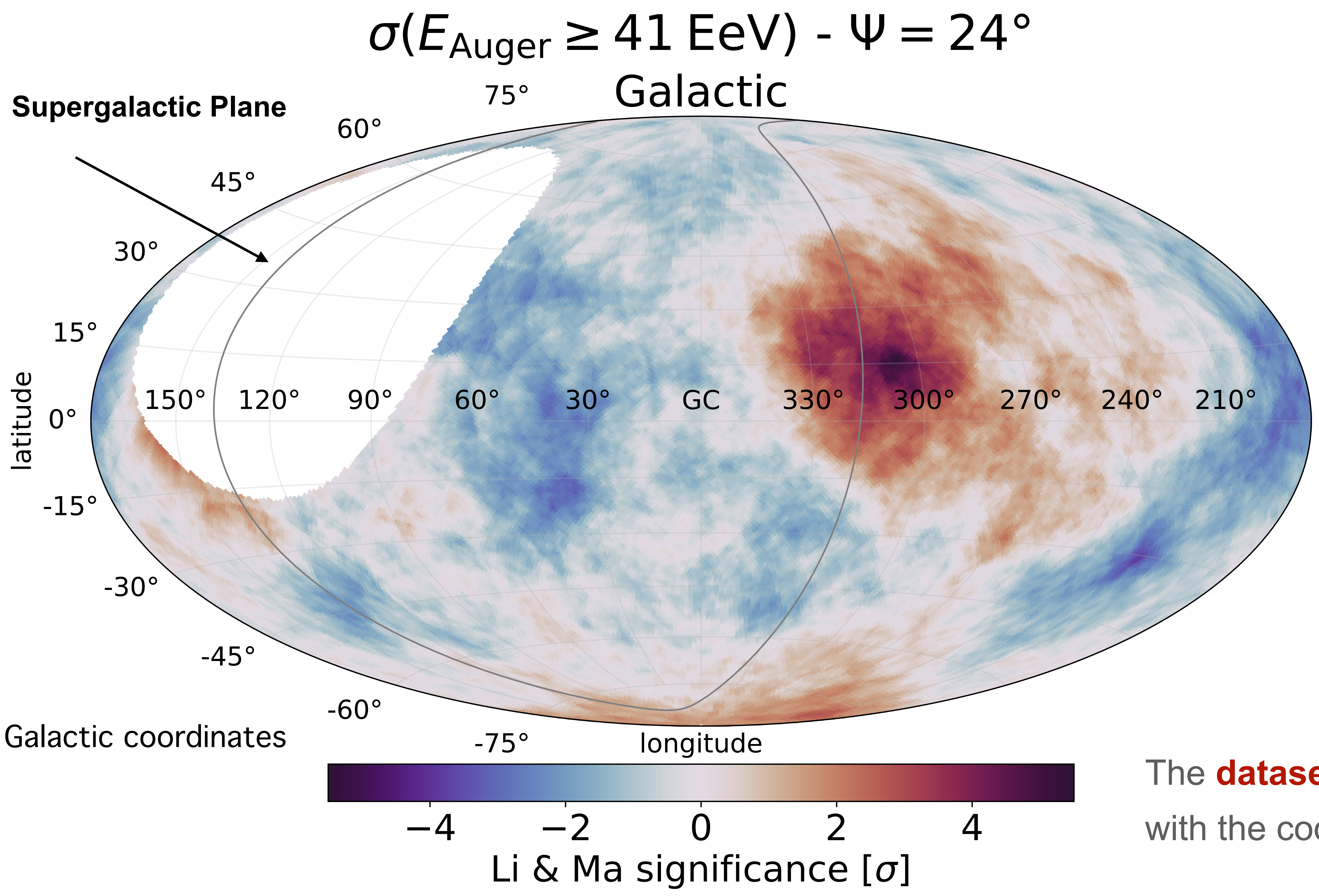

Approach

- Investigate binomial probability to measure the cumulative number of events (Nobs) given the expected on average from isotropic simulations (Nexp)
- **Scan in energy threshold in [32; 80] EeV, step of 1 EeV**
- **Scan in top-hat search angle Ψ in [1°; 30°], steps of 1°**

Most significant local excess over whole observable sky

$E_{th} \geq 41$ EeV, $\Psi = 24°$

$(\alpha, \delta) = (196.3°, -46.6°)$, $(l, b) = (305.4°, 16.2°)$

Nobs = *153* events, Nexp = *97.7* events from isotropy

Local *p*-value 3.7×10^{-8}, Li&Ma significance = 5.4σ

Global *p*-value = 3%
(after accounting the scan, penalty factor $\sim O(10^5)$)

The **dataset above 32 EeV is available for public use** with the code to reproduce the results (here)

(see Mario Buscemi's talk yesterday)

Excess in the Centaurus region

Method: Fix Centaurus A direction

► Compare the cumulative number of events (Nobs) with the expected on average from simulations assuming isotropy (Nexp)

► Compute the cumulative binomial probability to measure Nobs given Nexp

► **Scan in energy threshold in step of 1 EeV, top-hat search angle Ψ in [1°; 30°] in steps of 0.25° up to 5°, 1° for larger angles**

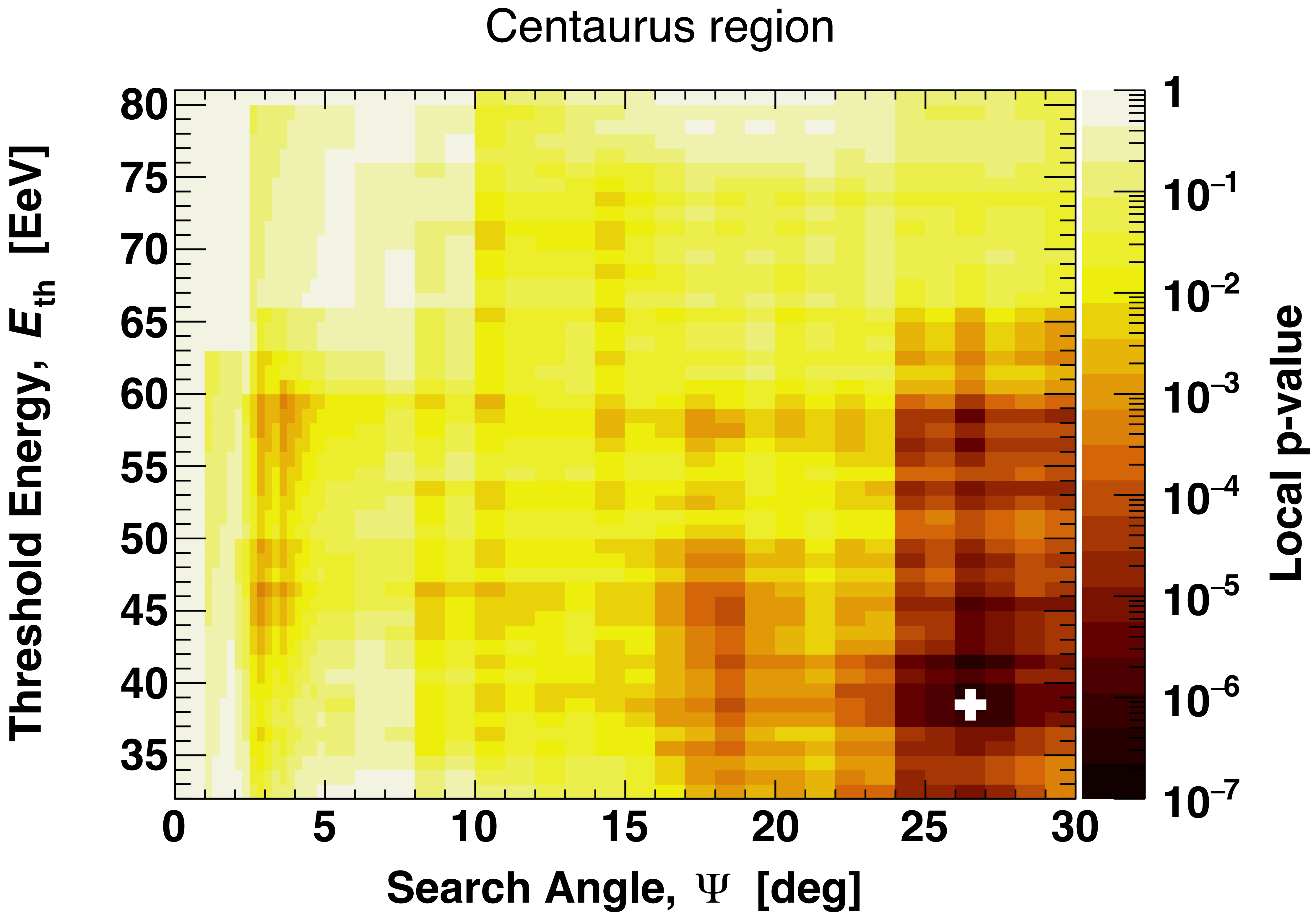

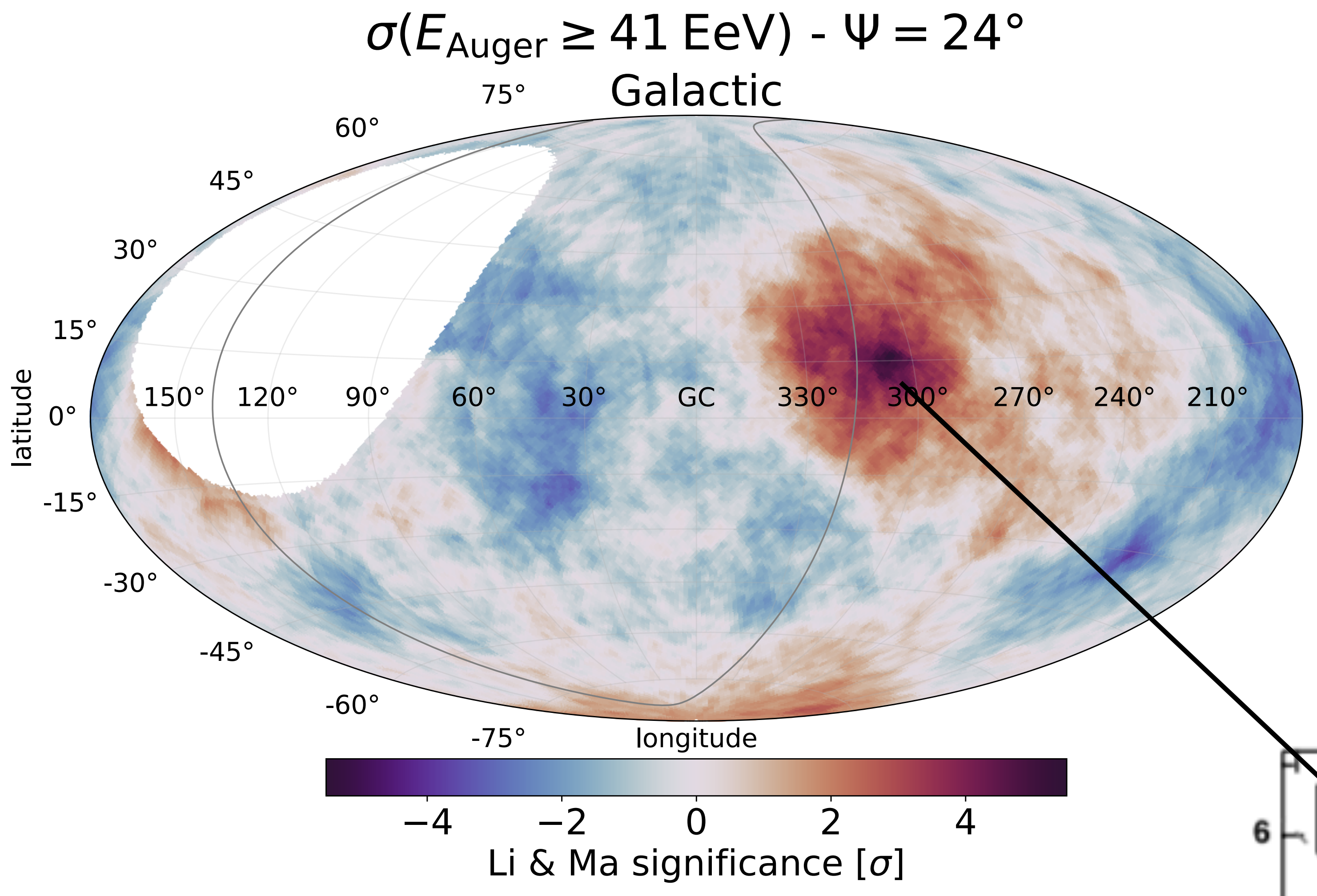

Crowed region in the Local Group

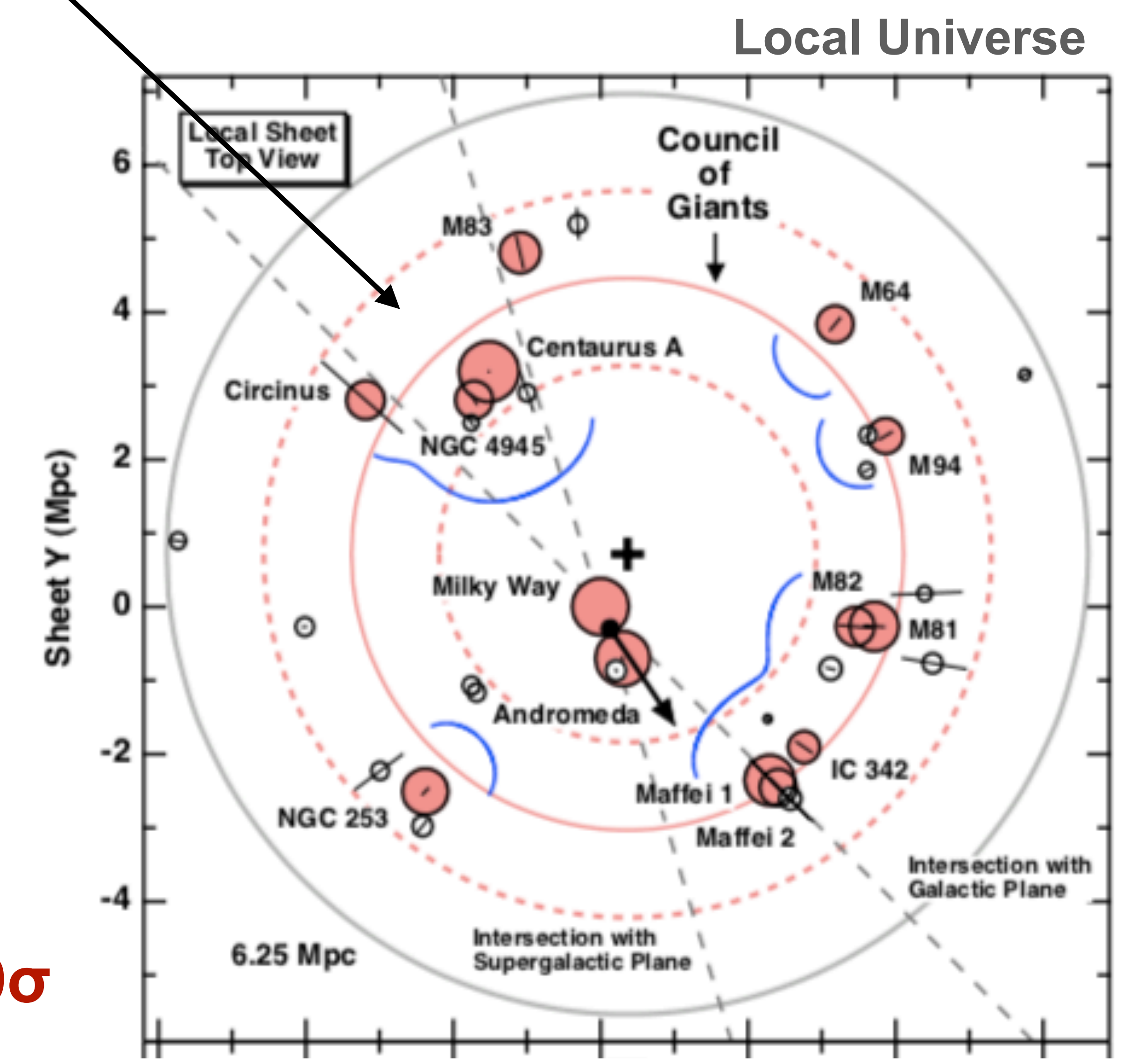

M. L. McCall Astrophys. J. 891 (2020) 142

Most significance excess

$E_{th} \geq 41$ EeV, Ψ = 27°

Nobs = 215, Nexp = 152

Local *p*-value 2.1×10^{-7}

Global p-value 4.5×10^{-5}, significance 3.9σ
(after accounting the scan)

⟹ search for correlation with extragalactic objects

Selection of non thermal sources

Four flux-limited catalogs - Jetted AGNs, all AGNs, Starburst galaxies, all galaxies

all galaxies from 2MASS

Assumption: UHECR flux ∝ stellar mass

Generic/stellar mass = IR from 2MRS (>40,000 galaxies 2.16 μm)

All AGNs observed with Swit-BAT

Assumption: UHECR flux ∝ hard-X rays flux

Accretion = X-rays from SwiftBAT (523 galaxies at 14-195 keV)

Starburst galaxies from JCAP, 2019 073 (Lunardini at al)

Assumption: UHECR flux ∝ star-forming activity

Burst = radio from Lunardini+19 (44 galaxies, 1.4 GHz)

Jetted AGNs from Fermi-LAT 3FHL catalog

Assumption: UHECR flux ∝ γ-rays flux

Jet = γ-rays from 3FHL (26 galaxies at 10 GeV-1 TeV)

Catalog-based searches

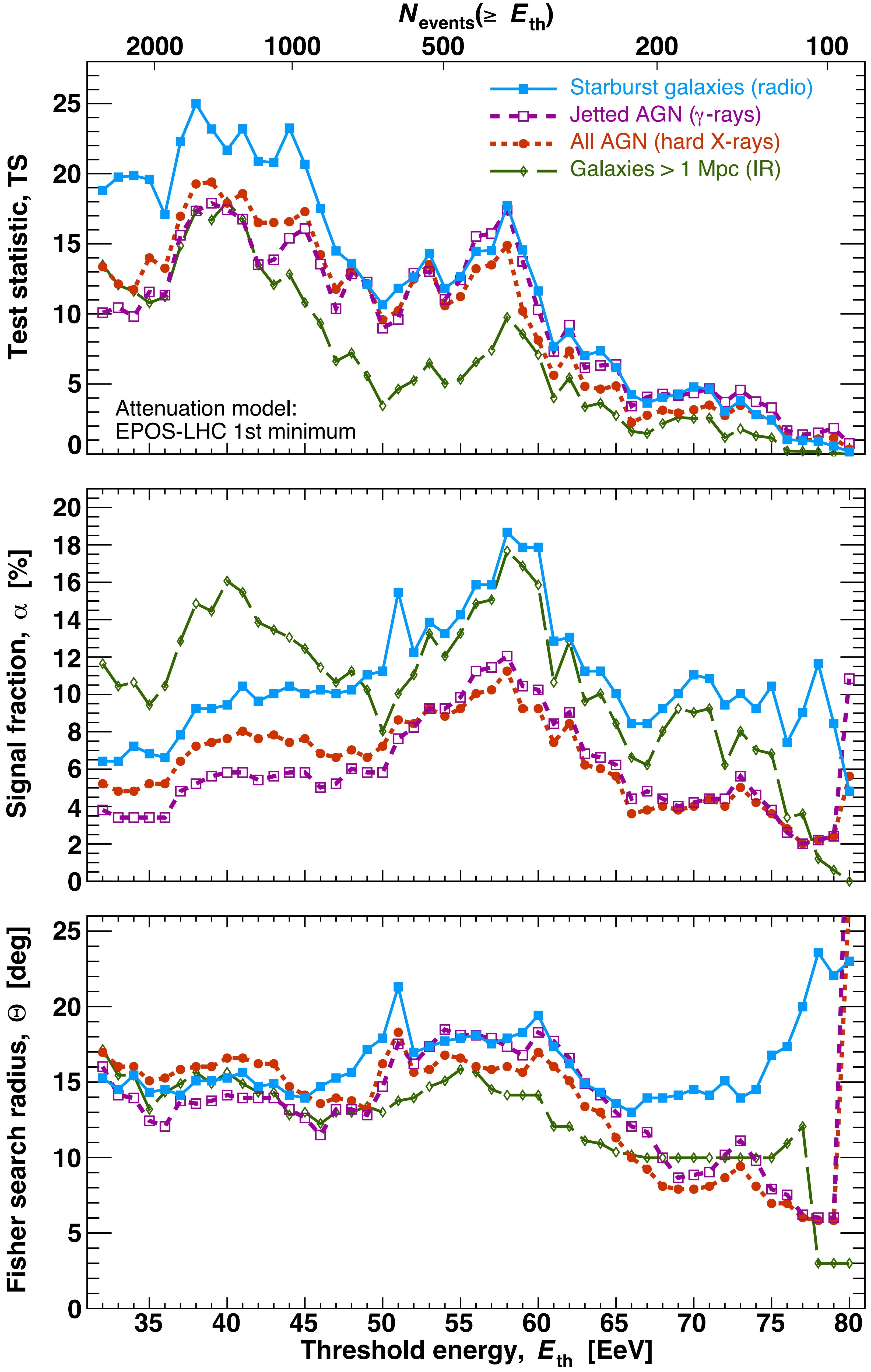

Pierre Auger Collab. The Astrophys. J. 935 (2022)170

Attenuation model: from best-fit escape spectrum of Auger spectral-composition modeling JCAP 03 (2018) E02

Method: Unbinned maximum likelihood analysis

UHECR sky model: isotropy + anisotropic component from candidate sources

Test statistic (TS) = LH ratio between H(UHECR sky model) and H(isotropy)

TS maximised vs Fisher search radius (Θ) and signal fraction (f) + energy scan

Best fit results at the global maximum

- **All galaxies, *E*th = 40 EeV, Θ = 16°, f = 16%, TS = 18.0, post-trial *p*-value = 7.9e−4 (3.2σ)**
- **Starburst, *E*th = 38 EeV, Θ = 15°, f = 9%, TS = 25.0, post-trial *p*-value = 3.2e−5 (4.0σ)**
- **All AGNs, *E*th = 39 EeV, Θ = 16°, f = 7%, TS = 19.4, post-trial *p*-value = 4.2e−4 (3.3σ)**
- **Jetted AGN, *E*th = 39 EeV, Θ = 14°, f = 6%, TS = 17.9, post-trial *p*-value = 8.3e−4 (3.1σ)**

Comparison with starburst galaxies indicate that isotropy is disfavored at a 4.0σ level (post-trial) but no preference with a specific class of galaxies can be stated

Comparing the sky models

Best fit model above 40 EeV

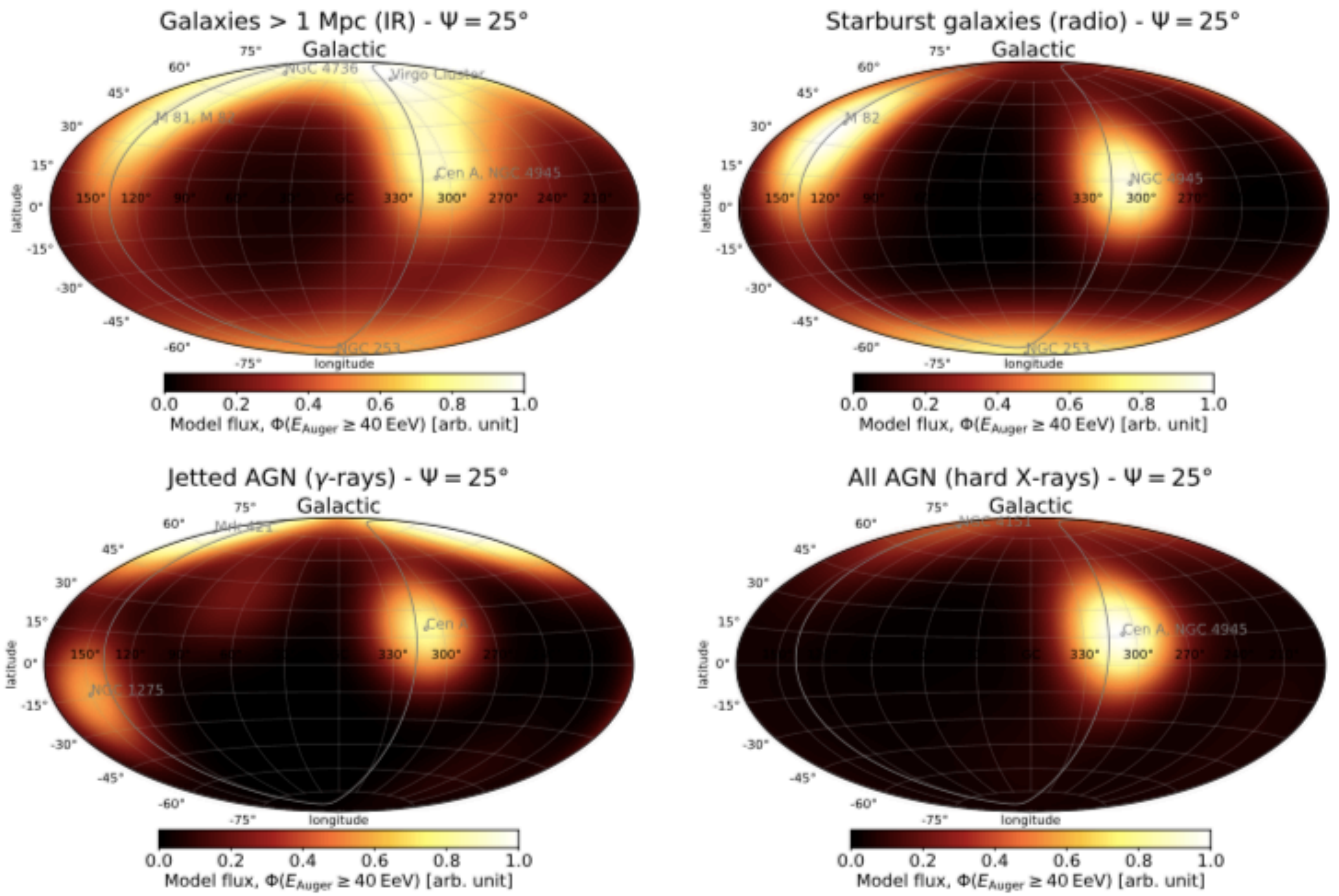

Observed above 41 EeV

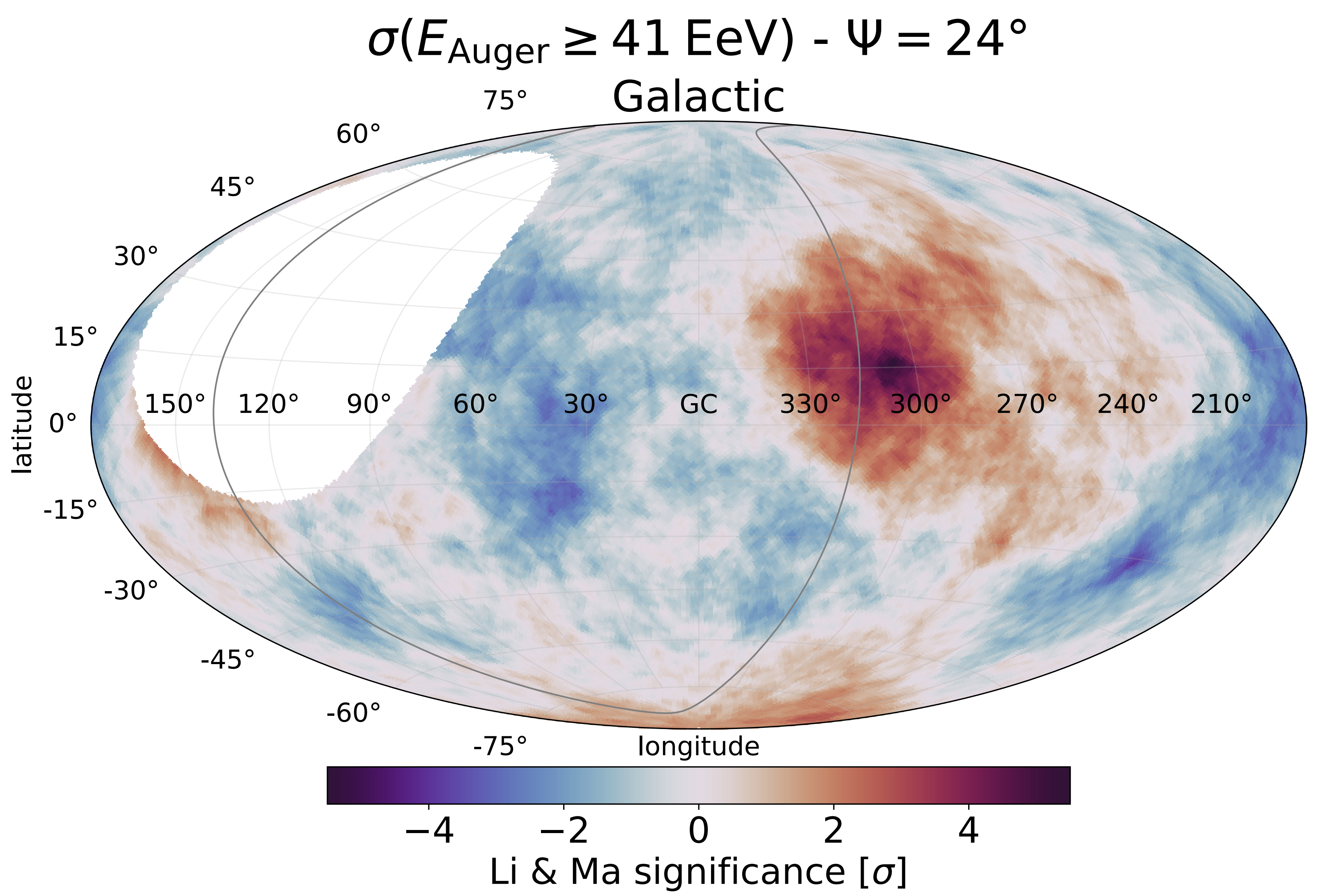

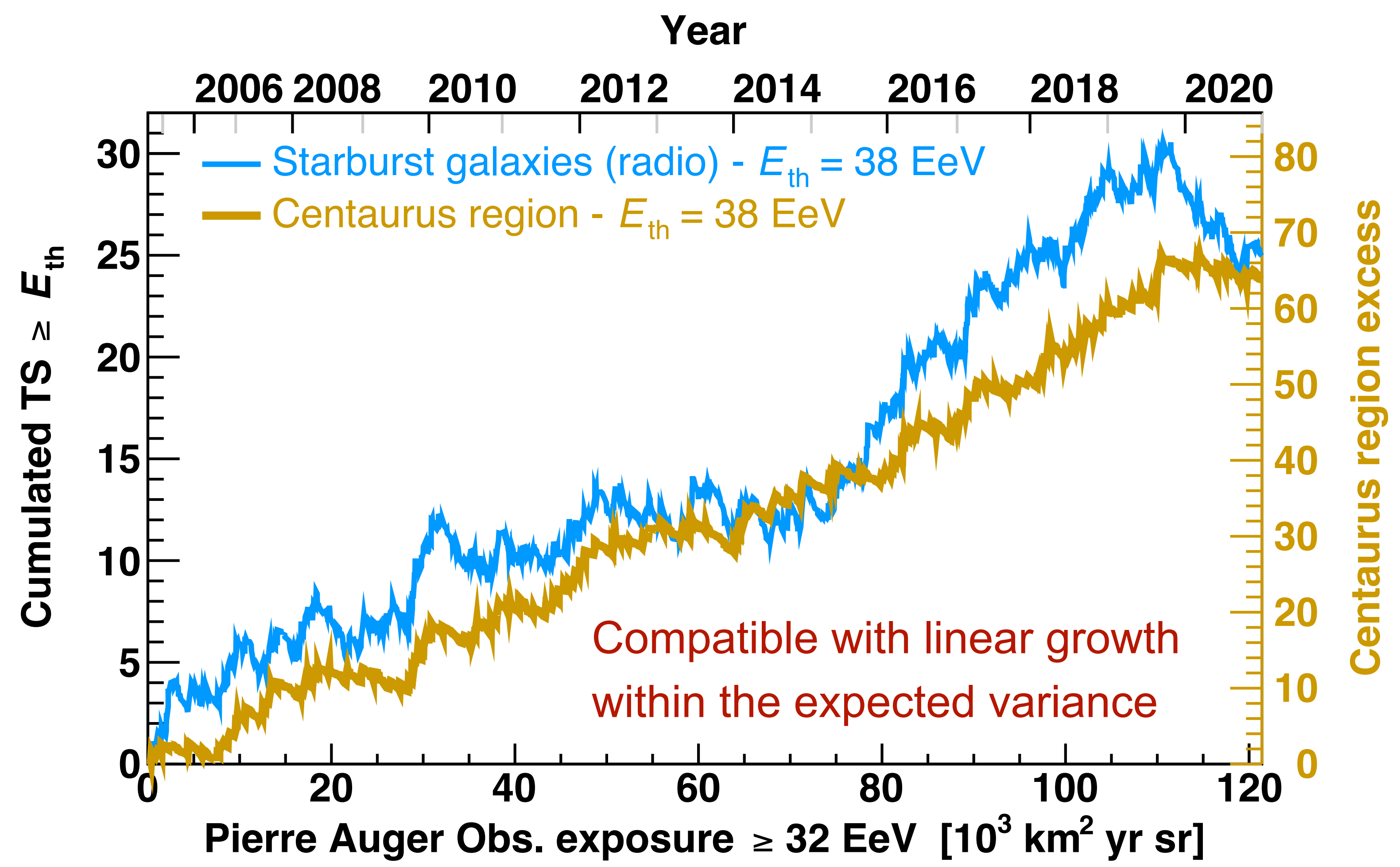

- All models capture the hotspot in the **Centaurus region** (M83+ NGC4945 + CenA)
- The starburst model adds the excess in the Galactic South Pole (NGC253)
- **5 sigma deviation from isotropy at 2025 ± 2 years** (165,000 ± 15,000 km^2 sr yr (C.L. 68%))

Conclusion and prospect with Auger Phase 1 data

1/2004 to 12/2020 ⟹ AugerPhase 1

Large scale anisotropy searches from below the 2nd knee up to the suppression region

- In the energy bin above 8 EeV, **evidence of departure from isotropy**
  ⟹ **first observational evidence that the origin of UHECRs is extragalactic**

The first evidence of anisotropy at UHE!

- Above 4 EeV, dipole amplitude grows with energy. Phases close to outer spiral arm
- For all the energy bins < 8 EeV, upper bound on equatorial dipole are at the level 1-3% at 99% CL
- Results on the right ascension phases suggest that the anisotropy has a predominantly Galactic origin below 1 EeV and a predominantly extragalactic origin above few EeV

Small-intermediate scale anisotropy searches in the suppression region

- **Indication of departure from isotropy** ~4σ from search in Centaurus region confirmed also by catalog-based searches
- Starburst galaxy model provides the most significant indication that UHECRs are not isotropically distributed
- The **dataset above 32 EeV is available for public use with the code to reproduce the results** (here)

The largest available dataset of ultra-high-energy cosmic rays above 32 EeV!

What comes next

"AugerPrime"

arXiv:1604.03637

Large and small scale anisotropy searches: keep collecting data (and controlling them!)

- Higher-order multipoles may appear with larger statistic?
- Confirm the SBGs-based anisotropy?
- Study relation between large to intermediate angular scale anisotropies
- Neutron searches
- Combined fit spectrum, Xmax and arrival directions (see Teresa Bister's poster)

Large scale anisotropy searches below 4 EeV down to the 2nd knee

- Search for large scale anisotropies in declination to probe the Galactic to extragalactic transition

The Pierre Auger Observatory is the only detector providing anisotropy measurements in this energy range

Large and small scale anisotropy searches: go to full sky above ~ 8 EeV

- With Telescope Array (as showed by Federico Urban in the Auger-TA WG report)

AugerPrime Program

- Looking at the sources using energies, positions and mass composition of the observed events (see Corinne Bérat's talk this afternoon and Tim Huege 's talk on Friday)
- Promising results including Xmax information (see Eric Mayotte's talk)

Extra slides

Another view

Flux sky map ***E*** **> 8 EeV**

GMF deflections [*Farrar 2012*]
for Z = 1.7÷ 5 [Pierre *Auger Collaboration PRD 90 (2014) 122006*]

Pierre Auger Observatory Science 357 (2017)

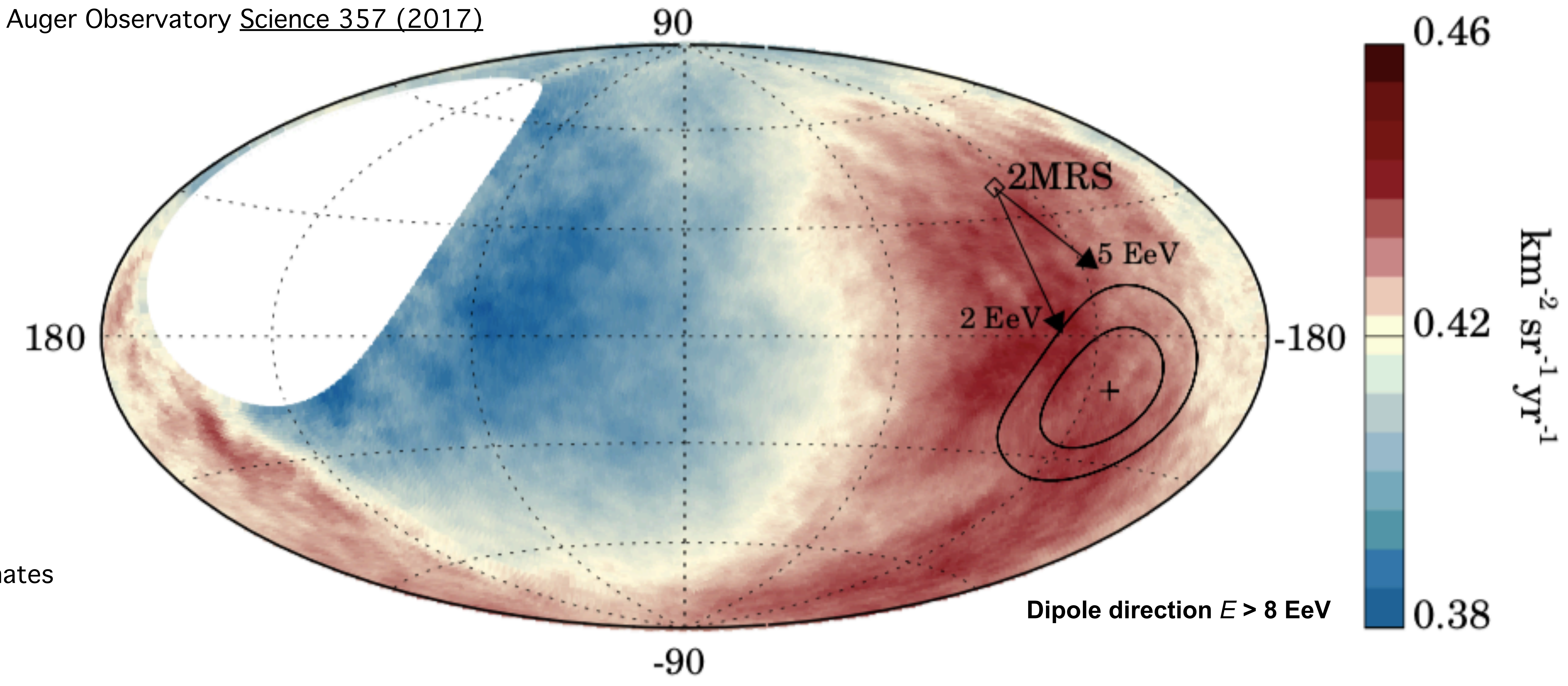

Galactic coordinates

Dipole direction ***E*** **> 8 EeV**

Dipole direction consistent at 2σ level with the 2MRS galaxies when CR composition inferred at these energies are assumed

Another view

Pierre Auger Collab. Astrophys. J. 891 (2020) 142

E > 0.25 EeV

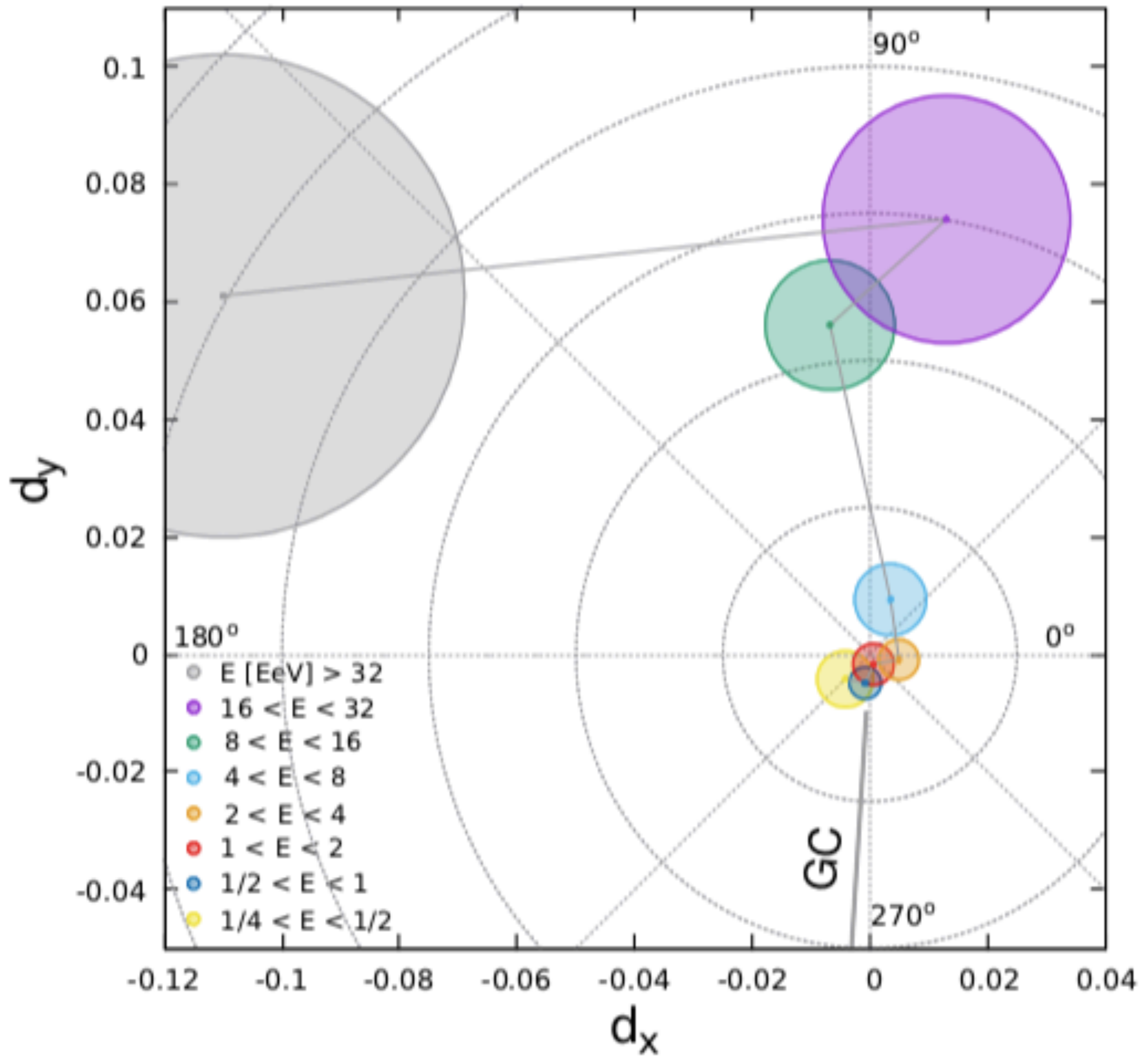

E < 0.25 EeV

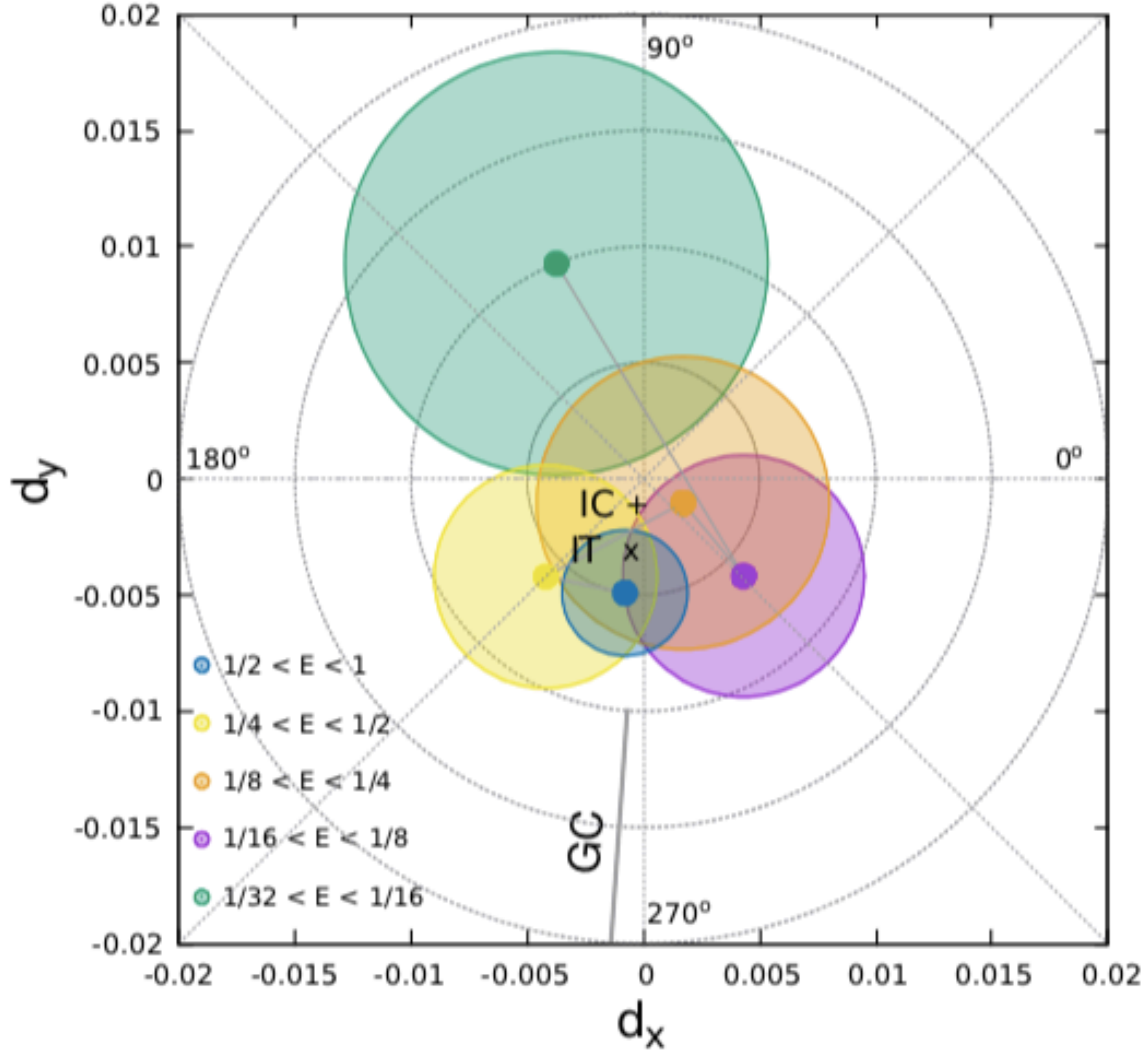

Equatorial dipole component above 0.03 EeV

	E [EeV]	$E_{\rm med}$ [EeV]	N	$d_\perp$ [%]	$\sigma_{x,y}$ [%]	$\alpha_d [^\circ]$	$P(\geq d_\perp)$	$d_\perp^{\rm UL}$ [%]
East-West	1/32 - 1/16	0.051	432,155	$1.0^{+1.0}_{-0.4}$	0.91	112 ± 71	0.54	3.3
(SD750)	1/16 - 1/8	0.088	924,856	$0.6^{+0.6}_{-0.3}$	0.52	-44 ± 68	0.50	2.0
	1/8 - 1/4	0.161	488,752	$0.2^{+0.8}_{-0.2}$	0.63	-31 ± 108	0.94	2.0
East-West	1/4 - 1/2	0.43	770,316	$0.6^{+0.5}_{-0.3}$	0.48	-135 ± 64	0.45	1.8
(SD1500)	1/2 - 1	0.70	2,388,467	$0.5^{+0.3}_{-0.2}$	0.27	-99 ± 43	0.20	1.1
	1 - 2	1.28	1,243,103	$0.18^{+0.47}_{-0.02}$	0.35	-69 ± 100	0.87	1.1
Rayleigh	2 - 4	2.48	283,074	$0.5^{+0.4}_{-0.2}$	0.34	-11 ± 55	0.34	1.4
(SD1500)	4 - 8	5.1	88,325	$1.0^{+0.7}_{-0.4}$	0.61	69 ± 46	0.23	2.6
	8 - 16	10.3	27,271	$5.6^{+1.2}_{-1.0}$	1.1	97 ± 12	2.3×10^{-6}	–
	16 - 32	20.3	7,664	$7.5^{+2.3}_{-1.8}$	2.1	80 ± 17	1.5×10^{-3}	–
	≥ 32	40	1,993	13^{+5}_{-3}	4.1	152 ± 19	5.3×10^{-3}	–
	≥ 8	11.5	36,928	$6.0^{+1.0}_{-0.9}$	0.94	98 ± 9	1.4×10^{-9}	–

Reconstruction of anisotropies beyond the dipole

Higher order multipoles (with small amplitudes) can also be present for a pure dipole at the entrance of the Galaxy

Without full sky coverage

$$\Phi(\alpha,\delta) = \sum_{l=0}^{l=\infty} \sum_{m=-l}^{l} a_{lm} Y_{lm}(\alpha,\delta)$$

Recovering power spectrum if Φ stationary

JCAP 0410 (2004) 008

$$c_l = \sum_{m=-l}^{l} \frac{a_{lm}^2}{2l+1}$$

Pierre Auger Collaboration
ICRC2021
JCAP 06 (2017) 026

Recovering coefficients if Φ bounded to lmax (l=2) allowing the presence of a quadrupolar moment

$$\Phi(\alpha,\delta) = \sum_{l=0}^{l=2} \sum_{m=-l}^{l} a_{lm} Y_{lm}(\alpha,\delta)$$

E > 8 EeV

$d_x = -0.001 \pm 0.011$	$Q_{zz} = 0.02 \pm 0.06$
$d_y = 0.06 \pm 0.01$	$Q_{xx} - Q_{yy} = 0.08 \pm 0.04$
$d_z = -0.03 \pm 0.03$	$Q_{xy} = 0.02 \pm 0.02$
	$Q_{xz} = 0.02 \pm 0.03$
	$Q_{yz} = -0.003 \pm 0.026$

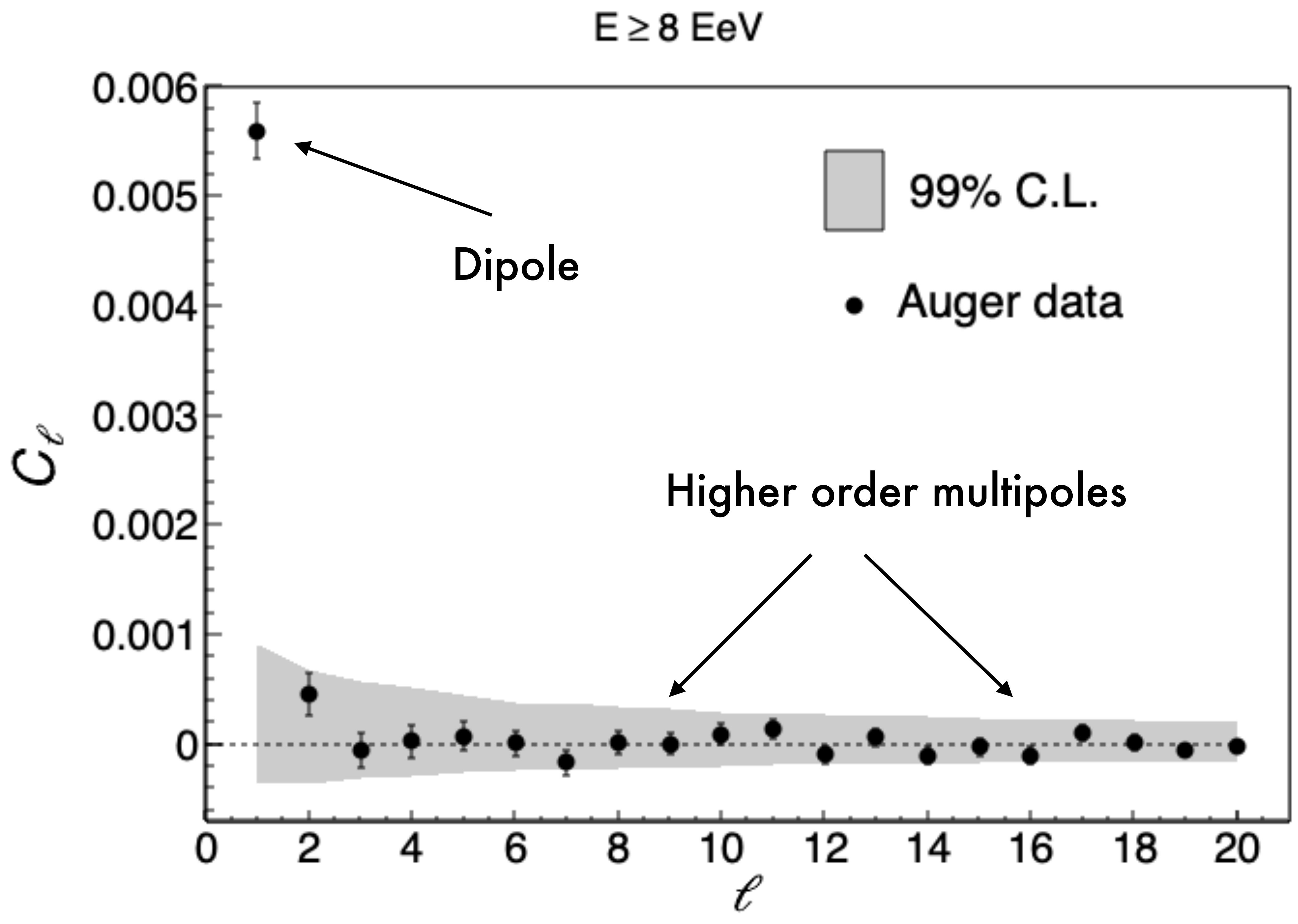

Quadrupolar amplitudes not significant, dipole components consistent with those obtained by assuming a pure dipole

Under stationarity assumptions no signal beyond the dipole moment

Catalog-based searches

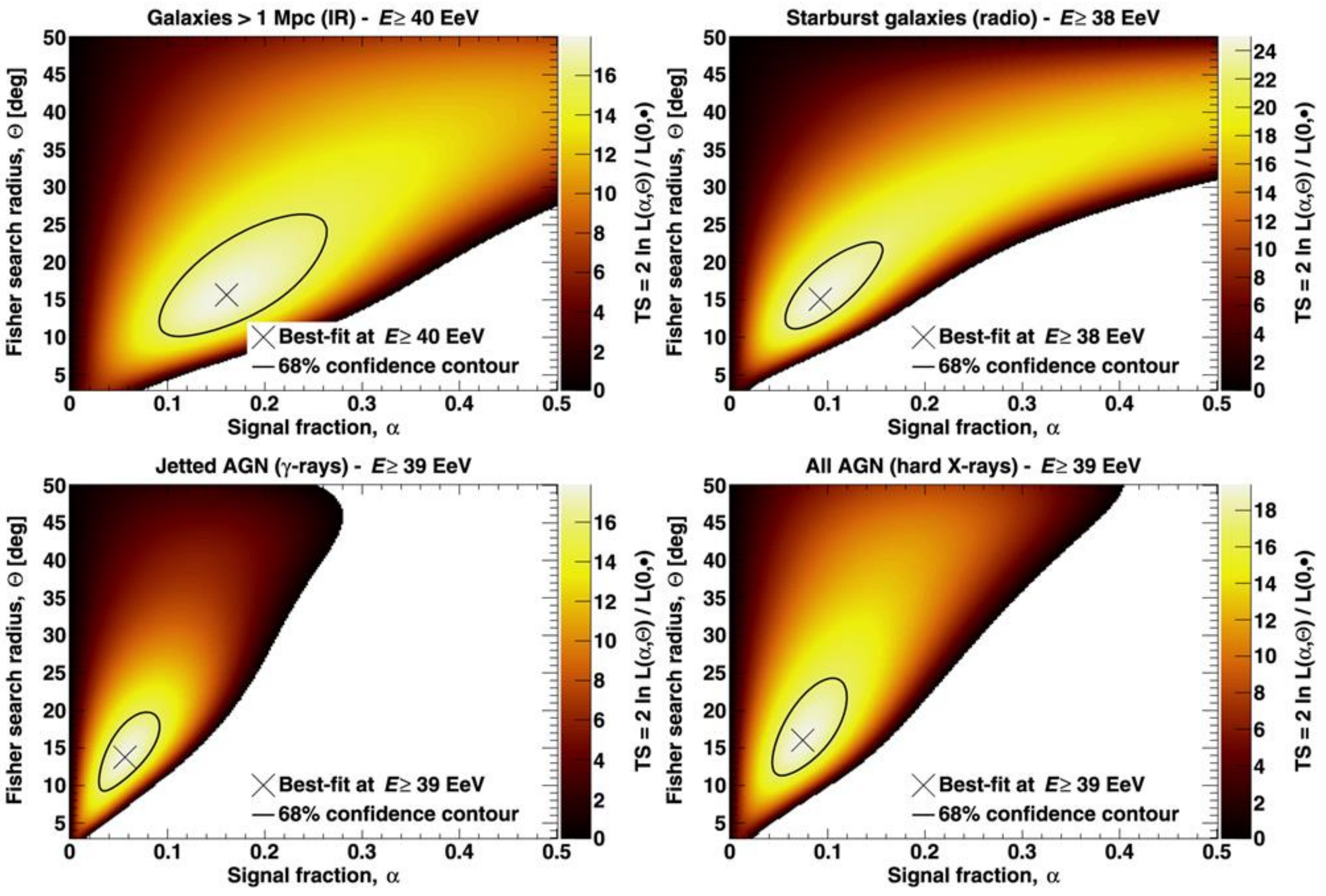

Global maximum

Best-fit Results Obtained with the Four Catalogs at the Global (Upper) and Secondary (Lower) Maximum

Catalog	E_{th} [EeV]	Fisher Search Radius, Θ [deg]	Signal Fraction, α [%]	TS_{max}	Post-trial *p*-value
All galaxies (IR)	40	16^{+11}_{-6}	16^{+10}_{-7}	18.0	7.9×10^{-4}
Starbursts (radio)	38	15^{+8}_{-4}	9^{+6}_{-4}	25.0	3.2×10^{-5}
All AGNs (X-rays)	39	16^{+8}_{-5}	7^{+5}_{-3}	19.4	4.2×10^{-4}
Jetted AGNs (γ-rays)	39	14^{+6}_{-4}	6^{+4}_{-3}	17.9	8.3×10^{-4}
All galaxies (IR)	58	14^{+9}_{-5}	18^{+13}_{-10}	9.8	2.9×10^{-2}
Starbursts (radio)	58	18^{+11}_{-6}	19^{+20}_{-9}	17.7	9.0×10^{-4}
All AGNs (X-rays)	58	16^{+8}_{-6}	11^{+7}_{-6}	14.9	3.2×10^{-3}
Jetted AGNs (γ-rays)	58	17^{+8}_{-5}	12^{+8}_{-6}	17.4	1.0×10^{-3}

Correlation with Structures

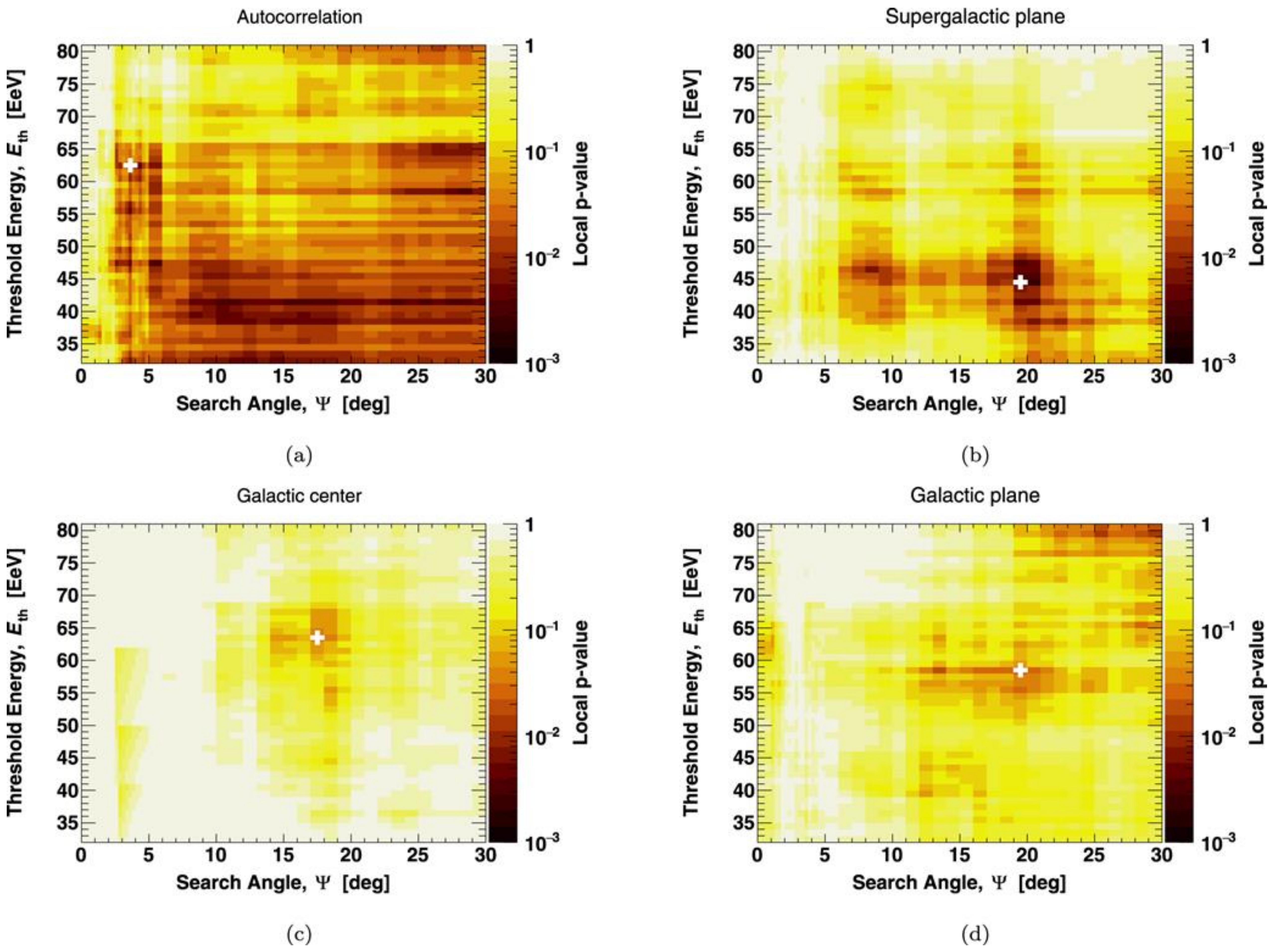

Table 1
Results of the Search for Autocorrelation and Correlation with Astrophysical Structures

Search	E_{th} [EeV]	Angle, Ψ [deg]	N_{obs}	N_{exp}	Local p-value, f_{min}	Post-trial p-value
Autocorrelation	62	3.75	93	66.4	2.5×10^{-3}	0.24
Supergalactic plane	44	20	394	349.1	1.8×10^{-3}	0.13
Galactic plane	58	20	151	129.8	1.4×10^{-2}	0.44
Galactic center	63	18	17	10.1	2.6×10^{-2}	0.57

Comparing the sky models

Best fit model above 40 EeV

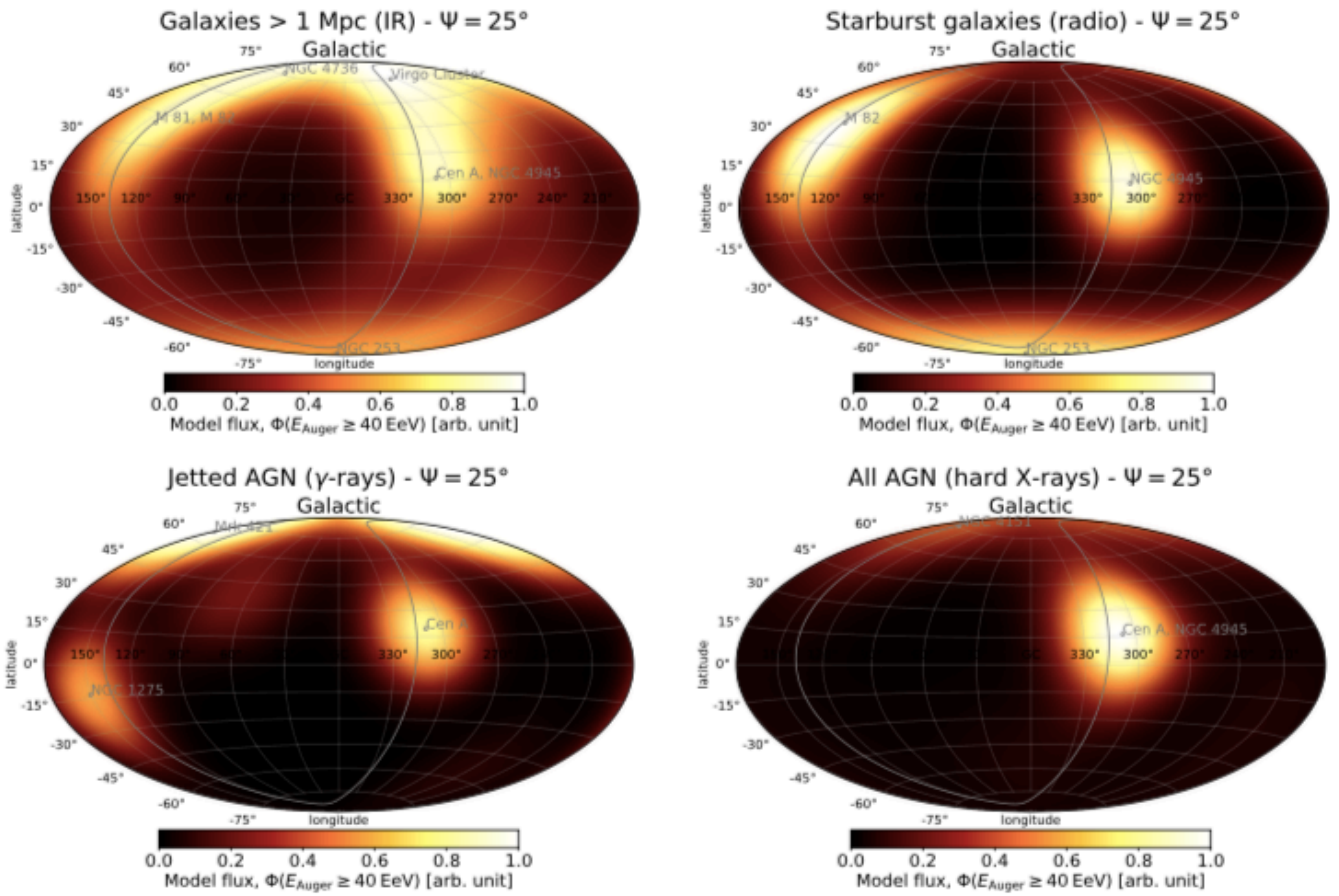

Observed above 41 EeV

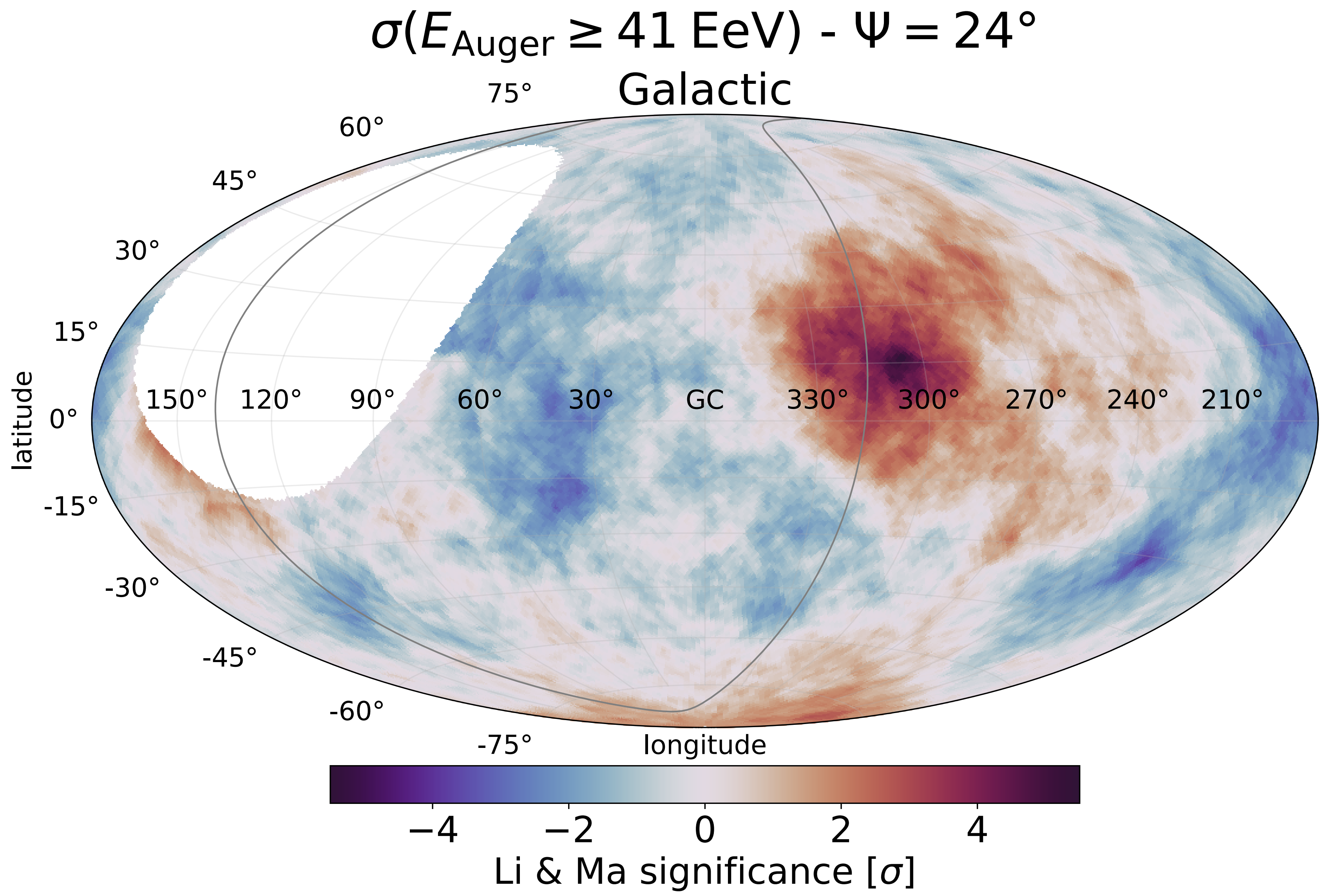

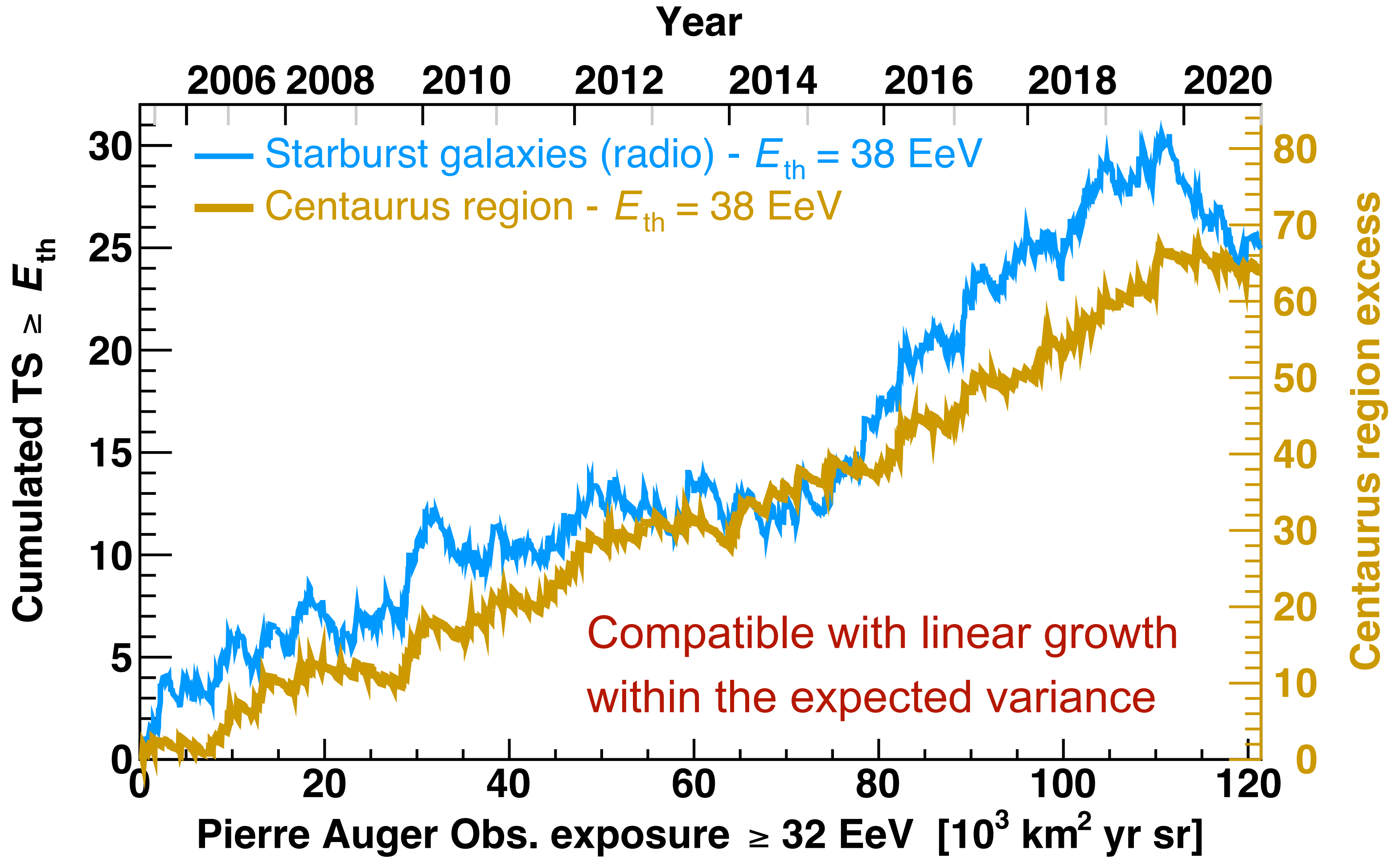

- All models capture the hotspot in the **Centaurus region** (M83+ NGC4945 + CenA)
- The starburst model adds the excess in the Galactic South Pole (NGC253)
- **5 sigma deviation from isotropy at 2025 ± 2 years** (165,000 ± 15,000 km^2 sr yr (C.L. 68%))

Starburst galaxies and Centaurus region

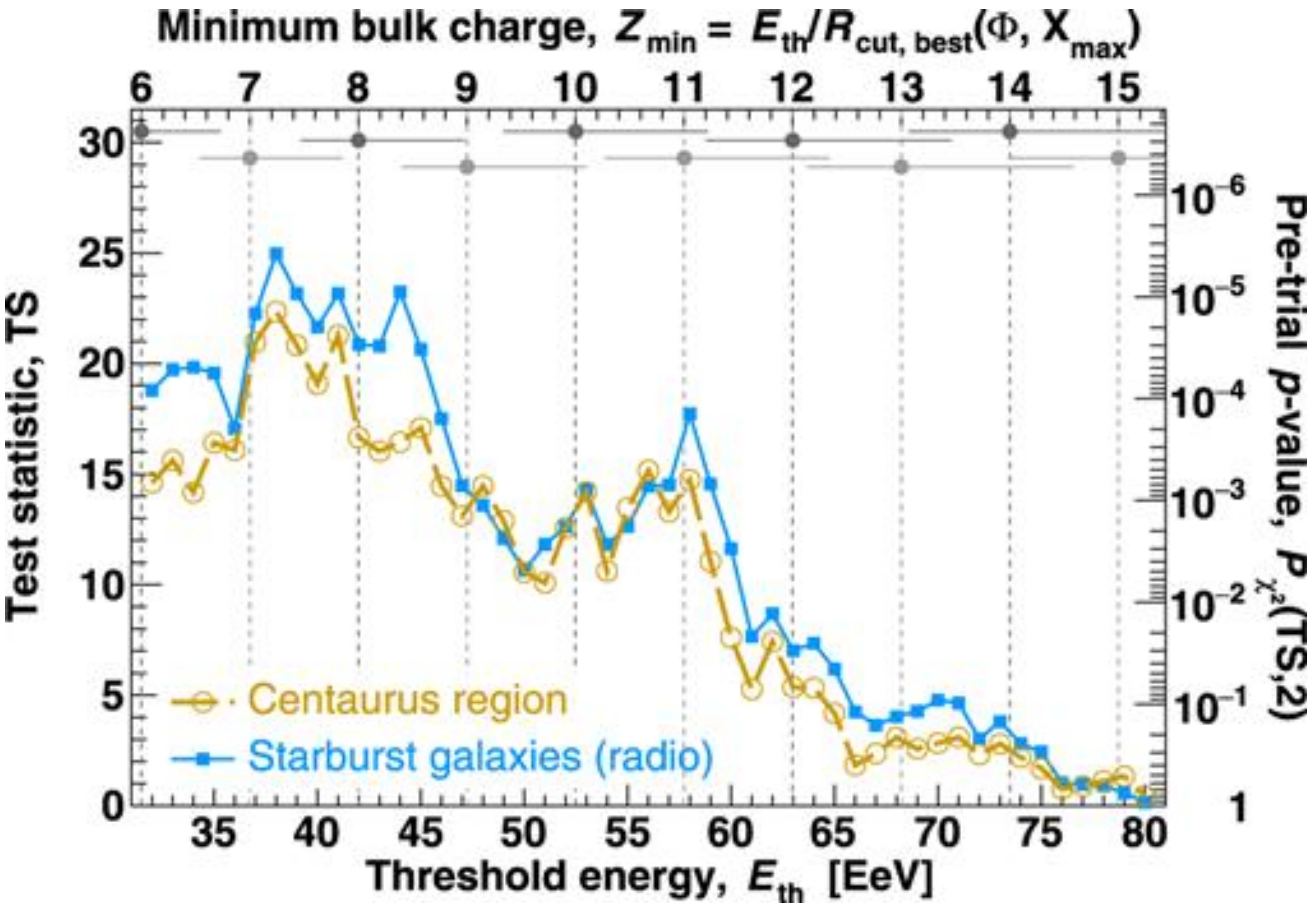

Evolution of the signal

Considering the best-fit parameters of the Centaurus region search

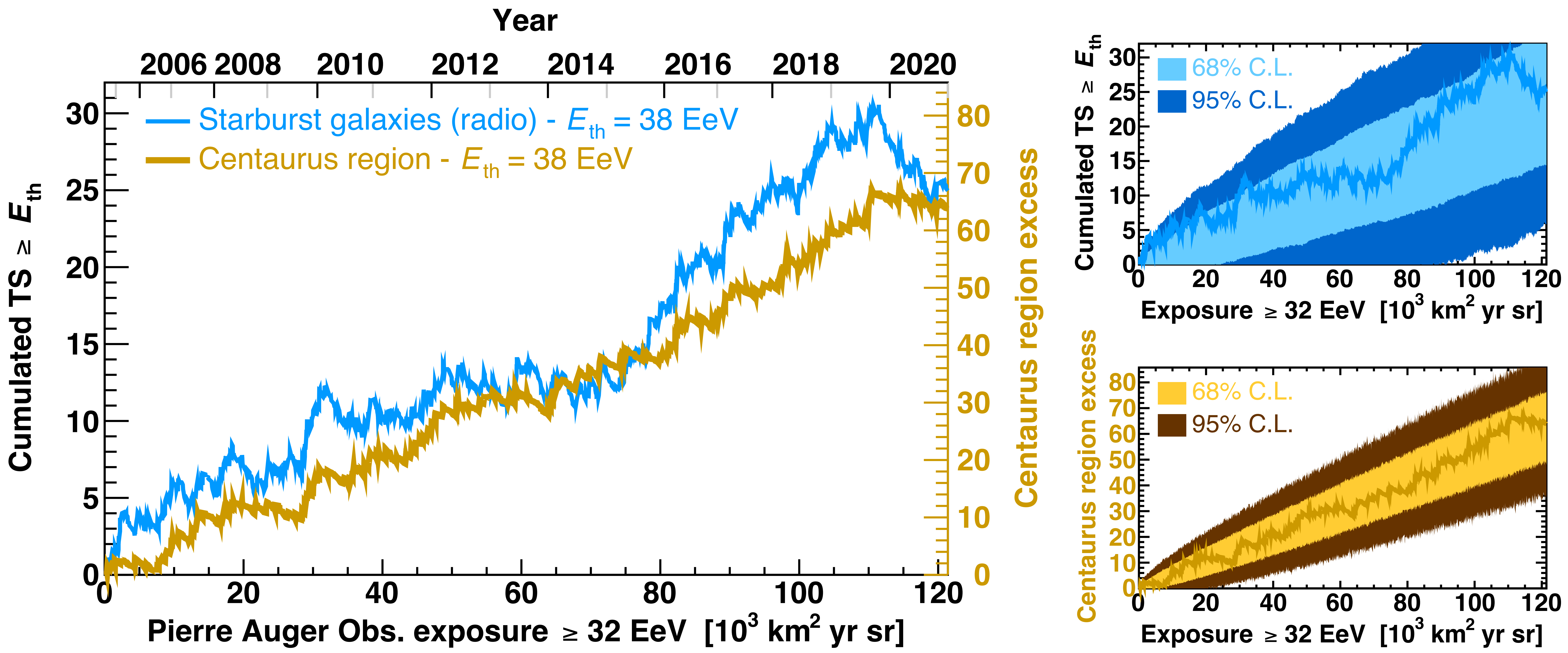

Compatible with linear growth within the expected variance

⟹ 5 sigma deviation from isotropy at 2025 ± 2 years